UNIVERZITA PALACKÉHO V OLOMOUCI

Přírodovědecká fakulta

Katedra biochemie

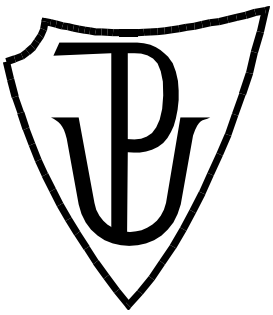

Charakterizace vlivu strigolaktonů na organizaci a dynamiku rostlinného cytoskeletu

BAKALÁŘSKÁ PRÁCE

Autor:	**Sofiia Hlynska**
Studijní program:	B1406 Biochemie
Studijní obor:	Biotechnologie a genové inženýrství
Forma studia:	Prezenční
Vedoucí práce:	**Yuliya Krasylenko, PhD**
Rok:	2020

PALACKY UNIVERSITY OLOMOUC

Faculty of Science

Department of Cell Biology

Characterization of strigolactone effects on plant cytoskeleton organization and dynamics

BACHELOR THESIS

Author:	**Sofiia Hlynska**
Study programme:	B1406 Biochemie
Field of study:	Biotechnology and Genetic Engineering
Form of study:	Full
Supervisor:	**Yuliya Krasylenko, PhD**
Year:	2020

Prohlašuji, že jsem bakalářskou práci vypracovala samostatně s vyznačením všech použitých pramenů a spoluautorství. Souhlasím se zveřejněním bakalářské práce podle zákona č. 111/1998 Sb., o vysokých školách, ve znění pozdějších předpisů. Byla jsem seznámena s tím, že se na moji práci vztahují práva a povinnosti vyplývající ze zákona č. 121/2000 Sb., autorský zákon, ve znění pozdějších předpisů.

V Olomouci dne .....……...

I declare that I developed this bachelor thesis separately with showing all the sources and authorship. I agree with the publication of the thesis by Act no. 111/1998 Coll., about universities, as amended. I was awared of that the rights and obligations arising from the Act no. 121/2000 Coll., the Copyright Act, as amended, are applied to my work.

In Olomouc ……...……

Poděkování

Nejprve bych ráda poděkovala své vedoucí Dr. Yuliyi Krasylenko za vše, co mě naučila během mé bakalářské práce. Zvláště oceňuji, že mi poskytla mnohem více možností, jak se v oblasti vědecké práce rozvíjet, než se studentům obvykle dostává. Dále bych chtěla upřímně poděkovat doc. George Komisovi za jeho přátelský přístup, mikroskopický výcvik, cenné návrhy a neustálou pomoc s přípravou mé bakalářské práce. Určitě chci také vyjádřit své uznání pro doc. Komise a Mgr. Terezu Vavrdovou za jejich příspěvky k některým měřením a statistické analýze mých primárních dat. Velmi si cením všech lidí z Oddělení buněčné biologie za vytvoření inspirativní pracovní atmosféry.

Acknowledgements

First, I would like to thank to my supervisor Dr. Yuliya Krasylenko for all things she taught me during my work on a bachelor thesis. I especially appreciate that she provided me much more possibilities to develop myself in a field of science work than students usually have. Next, I would like to thank sincerely to doc. George Komis for his friendly attitude, microscopy training, valuable suggestions and constant help with my bachelor thesis preparation. Surely, I want to acknowledge both doc. Komis and Mgr. Tereza Vavrdová for their contribution to some of the measurements and the statistical analysis of my primary data. I deeply appreciate all people from the the Department of Cell Biology for the creation of an inspiring working atmosphere.

Bibliografická identifikace

Jméno a příjmení autora	Sofiia Hlynska
Název práce	Charakterizace vlivu strigolaktonů na organizaci a dynamiku rostlinného cytoskeletu
Typ práce	Bakalářská
Pracoviště	Oddělení Buněčné Biologie
Vedoucí práce	Yuliya Krasylenko, PhD
Rok obhajoby práce	2020

Abstract

V této bakalářské práci je zkoumána role nedávno identifikované třídy fytohormonů, strigolaktonů ve formování architektury hypokotylu *Arabidopsis* prostřednictvím cytoskeletového přeuspořádání. Pro lepší pochopení působení strigolaktonu na buněčné úrovni, jsme studovali účinky exogenně aplikovaného syntetického analogu strigolaktonu ± GR24 a inhibitoru biosyntézy strigolaktonu TIS108 na organizaci kortikálních mikrotubulů a aktinových vláken v epidermálních buňkách vystavených působení světla a etiolovaných hypokotylů WT a necitlivému k strigolaktonu *Arabidopsis* mutantu *max 2-1* pomocí laserové skenovací konfokální mikroskopie a rotující diskové mikroskopie. Na základě našeho zjištění, je to první práce, která ukazuje účinky strigolaktonu na organizaci kortikálních mikrotubulů a aktinových vláken v rostlinných buňkách. Bylo zjištěno, že strigolaktony modulují cytoskeletální remodelaci během inhibice elongace hypokotylu světelně závislým způsobem.

Klíčová slova	Strigolactony, světlo, rostlinný cytoskelet, kortikální mikrotubuly, aktinová vlákna, cytoskeletální organizace, etiolované hypocotyly, CLSM, SIM, spinning disk, *Arabidopsis thaliana, max2-1* mutant
Počet stran	70
Počet příloh	1
Jazyk	Anglický

Bibliographical identification

Autor's first name and surname	Sofiia Hlynska
Title	Characterization of strigolactone effects on plant cytoskeleton organization and dynamics
Type of thesis	Bachelor
Department	Department of Cell Biology
Supervisor	Yuliya Krasylenko, PhD
The year of presentation	2020

Abstract

In this bachelor thesis, we addressed the role of the recently identified class of phytohormones, strigolactones, a recently identified class of plant hormones in hypocotyl growth inhibition by virtue of strigolactone induced cytoskeletal remodeling. For this purpose, the synthetic strigolactone analogue ±GR24 and the inhibitor of strigolactone biosynthesis TIS108 were used to treat *Arabidopsis* seedlings and subsequently study their effects on the organization of microtubules and actin microfilaments in epidermal cells of light-exposed and etiolated hypocotyls of WT and SL-insensitive signaling *Arabidopsis* mutant *max2-1* using laser scanning confocal microscopy and spinning disk microscopy. To our knowledge, this is the first report showing strigolactone effects on the organization of cortical microtubules and actin filaments in plant cells. It was found that strigolactones affect cytoskeletal remodeling during inhibition of hypocotyl elongation in a light-dependent manner.

Keywords	Strigolactones, light, plant cytoskeleton, cortical microtubules, actin filaments, cytoskeletal organization, etiolated hypocotyls, CLSM, SIM, spinning disk, *Arabidopsis thaliana*, *max2-1* mutant
Number of pages	70
Number of appendices	1
Language	English

Content

Aims of the bachelor thesis

Theoretical part

In theoretical part I summarize the existing knowledge regarding the physiological functions of strigolactones in plants, structure and functional role of microtubules and actin filaments as components of plant cytoskeleton and their regulation by different classes of phytohormones.

Experimental part

The aim of the thesis is to study the role of strigolactones in the regulation of organization of cortical microtubules and actin filaments in light-exposed and etiolated *Arabidopsis* seedlings. The first goal is the phenotypic analysis of strigolactone effects on hypocotyl growth inhibition of *Arabidopsis* Col-0 and *max2-1* mutant and to address how strigolactone effects are modulated by the illumination conditions during seedling growth. The second goal is to study microtubule organization in epidermal hypocotyl cells of Col-0 and *max2*-1 seedlings stably expressing the MAP4-GFP and TUA6-GFP microtubule markers using confocal laser scanning microscopy (CLSM). The third goal is the characterization of the organization (occupancy and skewness) of F-actin in hypocotyl epidermal cells of light-exposed and etiolated *Arabidopsis* lines transformed with the Lifeact-GFP and fABD2-GFP actin markers using spinning disk microscopy.

1. INTRODUCTION

Phytohormones affect a lot of various aspects in plant morphogenesis. Such plant hormones as auxins, cytokinins, gibberellins, ethylene, abscisic, jasmonic and salicylic acids regulate plant growth, cell division, nutrients storage and other crucial processes as well as the defense strategies against pathogens and multiple abiotic stress environmental factors. Strigolactones as a novel class of phytohormones were discovered more than a decade ago as trace compounds just promoting parasitic plants germination, and until nowerdays the clarification of their role in plant devevopment requires jointed efforts of plant physiologists, cell, molecular biologists, biochemists and other specialists (Cheng et al., 2013). One of the important strigolactones' functions in higher plants is the stimulation of symbiotic interactions with arbuscular mycorrhizal fungi and the increase of the shoot branching (Waters et al., 2017). This discovery attracted an attention of private entrepreneurs such as Elon Mask to the investment into the future „space farming", since it is supposed that strigolactone hyperproducers would be able to thrive in the low-nutrient soil despite the microgravity conditions. The challenge of the sustainable cultivation of productive crops *in situ* under controlled conditions during long-term human space expeditions in the future would gain special attention of plant biologists. Hence, the understanding of the precise cellular mechanisms of the regulation of plant morphogenesis by strigolactones might allow to manipulate this process using genetic engineering and biotechnology instruments for the agriculture of the future. My thesis is focused on microtubules and actin filaments – the key components of plant cytoskeleton, a dynamic organelle with a plethora of fundamental functions such as cell motility, division, growth, polarity, microcompartmentalization, scaffolding and many others. Despite the effects of the „classical" phytohormones on the organization of cortical microtubules are known for years in details, regarding strigolactones the gap exists.

This thesis is dedicated to light-dependent remodeling of plant cytoskeleton in epidermal hypocotyls cells of model plant *Arabidopsis thaliana*. It is noteworthy that during the preparation of my thesis, I studied also the effects of GR24 and TIS108 on mitotic indices (whole-mounts and tubulin immunolabeling), cell division planes shifting (FM 4-64 staining) and EdU incorporation into the cells of primary roots, what are supposed to be continued in my further research.

2. CURRENT STATE OF THE TOPIC

2.1 Strigolactones as a novel class of plant hormones

Strigolactones (SL) are recently found carotenoid-derived plant hormones and rhizosphere signaling molecules from the group of terpenoid lactones (Zwanenburg and Pospíšil, 2013; Koltai, 2014). Initially, SL were discovered in the course of exogenous allelochemical responses as germination stimulants of the root parasitic weeds (witchweeds (*Striga* spp.), broomrapes (*Orobanche* and *Phelipanche* spp.) and the hemi-parasitic *Alectra* spp. (Gomez-Roldan et al., 2008).

2.1.1. Physiological functions of strigolactones in higher plants

In general, the endogenous physiological effects of SL on the aboveground plant part include the regression of plant height and hypocotyl length (Stirnberg et al., 2002; de Saint Germain et al., 2013) as well as auxin-mediated regulation of shoot branching (Kapulnik et al., 2011; Shinohara et al., 2013). SL increase of cotyledon expansion in dark-grown wild-type seedlings (Stirnberg et al., 2002; Tsuchiya et al., 2010), suppress the preformed axillary bud outgrowth (Gomez-Roldan et al., 2008; Umehara et al., 2008; Domagalska et al., 2011) and negatively regulate cell division in rice mesocotyls during germination and growth in darkness (Hu et al., 2010). Moreover, SL promote secondary growth and cell divisions in the cambium, stimulate leaf senescence (Agusti et al., 2011; Koltai, 2014), control leaf blade size, petiole elongation, branching angle and stem diameter (Smith and Waters, 2012; Bennett et al., 2016).

Under standard growth conditions (16 h/8 h light/dark cycle, 22/18°C), *Arabidopsis thaliana max4-5* mutants exhibited increased shoot branching, narrower branching angle, shorter height, reduced stem diameter and delayed leaf senescence as compared to WT of ecotype Columbia (Bennett et al., 2016). Recent studies suggest SL in low concentrations inhibit hypocotyl elongation in light-dependent manner. Assessment of SL effects on *Arabidopsis* WT and *max2* mutants showed that GR24, a synthetic SL, applied at concentrations below 10 μM, caused inhibition of hypocotyl growth on light rather than darkness, while *max2* mutants were nearly unresponsive to GR24 both on light and darkness (Jia et al., 2014). Furthermore, GR24 acts synergistically with auxins in the

processes of tuber formation and axillary stolon buds outgrowth, as well as in the promotion of the above-ground shoot branching in potato (Roumeliotis et al., 2012).

Recent studies showed that SL are also implicated in root development, since they inhibit lateral root formation (Kapulnik et al., 2011; Ruyter-Spira et al., 2011), negatively regulate adventitious root formation (Rasmussen et al., 2012), and stimulate primary root growth (Ruyter-Spira et al., 2011; 2013; Koren et al., 2013). Moreover, SL promote meristem cell number in the primary root in a MAX2-dependent manner (Koren et al., 2013; Ruyter-Spira et al., 2013), and mediate the phosphate- and nitrate-deficiency-induced root development and auxin transport in rice (Sun et al., 2014). Endogenous uptake of different synthetic SL analogues caused root hair elongation in WT and *max3*, *max4* SL deficient mutants of *Arabidopsis*, but it did not affect SL-unresponsive mutant *max2* (Kapulnik et al., 2011; Cohen et al., 2013). Apart from SL, the stimulation of root hair elongation is also mediated by ethylene and auxin (Kapulnik et al., 2011). In *Arabidopsis*, SL act to regulate the perception and the subsequent plant response to low phosphorus conditions (Kumar et al., 2015). SL also favour hyphal branching of arbuscular mycorrhizal fungi (Akiyama et al., 2005), promote nodulation in the legume-rhizobium symbiosis (Soto et al., 2010), and enhance plant resistance to drought, salt, osmotic stresses and low phosphate and nitrate content (Yoneyama et al., 2007; Foo et al., 2013; Ha et al., 2014). Finally, SL promote seed maturation and potentiate germination (Tsuchiya et al., 2010).

2.1.2. Variety of natural and synthetic strigolactones

Conventionally, SL usually have a butanolide ring (D-ring) connected to tricyclic lactone (ABC-rings) via an enol-ether bridge (Figure 1) (Lumba et al., 2017).

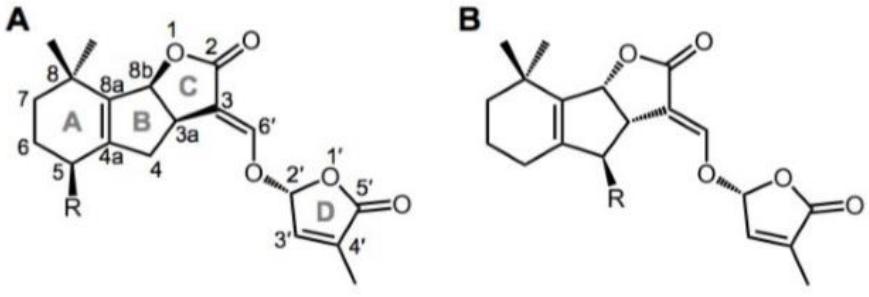

Figure 1. Chemical structure of strigolactones (SL). The chemical structures of naturally occurring SL can be divided into two families, the orobanchol (A) (R=H, 4-deoxyorabanchol; R = OH, orobanchol; R= OAc, orobanchol acetate) and strigol (B) (R=H, 5-deoxystrigol; R = OH, strigol; R = OAc, strigol acetate) basing on the stereochemistry around the BC (Lumba et al., 2017).

More than 20 naturally occurring SL were identified in root exudates present classified on the basis of the ABC ring stereochemistry. These SL are present at extremely low amounts and they include for example strigol in maize (*Zea mays* L.) and proso millet (*Panicum miliaceum* L.) as *Striga* host (Siame et al., 1993), sorgolactone in *Sorghum bicolor L.* Moench hosting *S. asiatica* and *S. hermonthica* (Hauck et al., 1992), and orobanchol in red clover (*Trifolium pretense* L.) hosting *Orobanche minor* (Yokata et al., 1998).

Apart from the naturally occurring SL species, synthetic ones have been also produced. One such is the generic SL analogue *rac*-GR24 (Johnson et al., 1981) comprising of two enantiomers (D14-perceived GR24+ and non-specific KAI2-recepted GR24-) is widely used artificial SL (Zwannenberg et al., 2013; Supplementary 1: Structure of synthetic SL analogue GR24 and inhibitor TIS108). More specific is the *cis*-GR24 consisting only of D14-perceived GR24+ (Zwannenberg et al., 2013). In this context, some SL-related phenotypes have been linked to specific stereoisoforms of *rac*-GR24 or specific receptors, although these observations were not absolute (Scaffidi et al., 2014; Conn et al., 2015; López-Ráez et al., 2017). Moreover, the number of synthetic SL is steadily increasing: CISA-1 (cyano-isoindole SL analogue) (Rasmussen et al., 2013), strigolactams (Lachia et al., 2015), nitro-phenlactones (Jia et al., 2016), series of carlactone-based compounds (Jamil et al., 2018, 2019) and MP16 (methyl phenlactonoate 16; Jamil et al., 2020).

2.1.3. Strigolactone biosynthesis and its inhibitors

In planta, SL are synthesized in plastids via carotenoid pathway starting from ß-carotene as a substrate for carotenoid-cleavage dioxygenase (CCD) enzymes (Saeed et al., 2017; Figure 2).

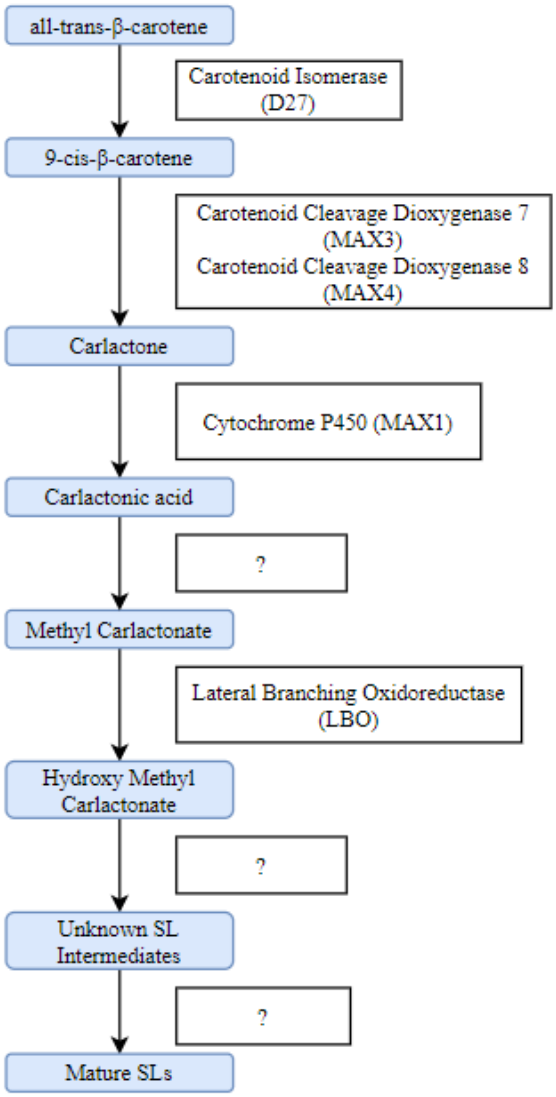

Figure 2. Strigolactone biosynthesis pathway (adapted from Claassens and Hills, 2018; Yoneyama, 2020).

CCDs form carbonyl compounds, so called apocarotenoids by specific cleavage of double bonds in carotenoids. The first step involves the conversion of all-trans-ß-carotene via the enzymatic function of 9-cis-ß-carotene isomerase ATD27 in *Arabidopsis* and its ortholog in rice DWARF27 (D27; Waters et al., 2017). Onwards 9-cis-ß-carotene is converted to carlactone by CCD7 and CCD8 (*max*2 and *max*3 mutants in *Arabidopsis* respectively; Saeed et al., 2017). CCD8 thereafter catalyzes the conversion not only to carlactone, but also hydroxy-carlactones (Yoneyama, 2020). The chemical formula of carlactone does not contain B ring and its structure includes only the A, C rings and enol-ether bond. This intermediated compound causes inhibition of shoot branching in

Arabidopsis and rice SL deficient mutants in addition it stimulates seed germination in holoparasitic plant *Striga hermonthica* (Abe et al., 2014; Seto et al., 2014). The next step is to oxidase carlactone to carlactonic acid (CLA) for a final conversion into mature SL (Brewer et al., 2016). An important enzyme of SL biosynthetic pathway is lateral branching oxidoreductase (LBO), which oxidase methyl carlactonoate to hydroxymethyl carlactonoate (1′-HO-MeCLA). After 1′-HO-MeCLA is converted by unknown enzymes to unknown intermediates on the way to mature SL (Yoneyama, 2020).

The carotenoid dioxygenases MORE AXILLARY GROWTH3 (MAX3; AtCCD7), MAX4 (AtCCD8) and the cytochrome P450 MAX1 (AtCyp711A1) were used to generate SL biosynthesis mutants (Turnbull et al., 2002; Sorefan et al., 2003; Booker et al., 2004, 2005; Auldridge et al., 2006). In turn, triazole- type inhibitors TIS108 (6-phenoxy-1-phenyl-2-(1H-1,2,4-triazol-1-yl) hexan-1) (Supplementary 2) and TIS13 (2,2-dimethyl-7-phenoxy-4(1H-1,2,4-triazol-1-yl)heptan-3-ol) targeted to cytochrome P450 enzyme have various physiological effects in *Arabidopsis* plants (Ito et al., 2013). Besides of inhibition of P450 monooxygenase, TIS13 inhibits the production of epi-5DS (5-Deoxystrigol), which is one of the stereoisomers of major naturally occurring SL in rice (Akiyama et al., 2010). Moreover, tebuconazole fungicide could be potential SL inhibitor, since it targets cytochrome P450 in fungi (Ito et al., 2013). Based on the transcriptome data, TIS108 might have some potential target sites at Cytochrome P450 and NADPH-cytochrome (Bao et al., 2017).

2.1.4. Strigolactones signaling and mutants

Like some other plant growth regulators such as jasmonate and gibberellins, the SL signaling machinery is involving proteosomal degradation, however, full pathway is not determined yet. SL are perceived via a specific receptor system that consists of several proteins including DWARF14 (D14) α/β-fold and F-box proteins designated MAX2/D3/RMS4, which are linked to a Skp, Cullin, F-box (SCF)-containing complex (reviewed by Kumar et al., 2015; Figure 3).

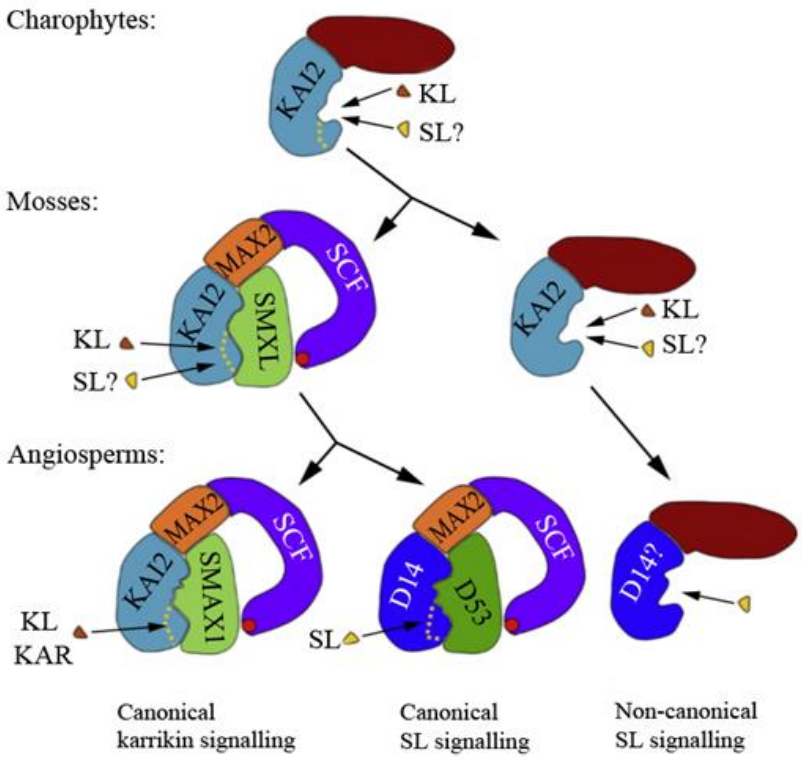

Figure 3. Hypothetical model of SL signaling. Binding of SL (yellow) to D14 α/ß-fold proteins cause a conformational change (dotted yellow line) that permits tight interaction of D14 (blue) and D53 chaperonin-like proteins (green) independently of MAX2 class F-box proteins (orange) (Bennett and Leyser, 2014).

One of the main components of SL signaling is D14 (DWARF14) α/ß-hydrolase protein derived from rice, and its *Arabidopsis* analogue At(14), petunia DAD2 and pea RMS4. In *Arabidopsis*, D14 interacts with the F-box and Leu-rich repeats protein MAX2 (MORE AXILLARY BRANCHING 2), and is probably acting either in SL signal perception or transduction via an ubiquitin-mediated degradation of target proteins (Ruyter-Spira et al., 2013; Bennett and Leyser, 2014; López-Ráez et al., 2017). MAX2 activity can be found in a broad spectrum of tissues (Stirnberg et al., 2007). Recent research in rice shows that the targets of D14-MAX2 tandem are members of the SMXL (SUPPRESSOR OF MAX2 1-LIKE) protein family (Soundappan et al., 2015). Minor deletion of 5 amino acids in SMLX family – DWARF53 (D53) (in *Arabidopsis* SMXL6,7,8) causes in SL-resistant plants with an increased branching phenotype. In turn, D53 is degraded in the presence of GR24 and this causes suppression of the dwarf and branched phenotypes. Hence, D53 proteins are targets for SL acting like a negative regulator of SL response (Zhou et al., 2013).

Additionally, SL signaling can be supported and overlap with the pathways of smoke-derived germination stimulants called karrikinns (KAI2) (Stanga et al., 2013). Karrikinns are the close family to D14/MAX2 involved in similar SL signaling pathways being negatively regulated by SMAX1 (SUPPRESSOR OF MORE AXILLARY GROWTH2 1 (Stanga et al., 2013). Several studies have started to address the effects of SL in cellular processes, including actin organization and dynamics (Pandya-Kumar et al., 2015); the distribution and membrane recycling of the PIN1 auxin efflux carrier of xylem parenchyma cells (Crawford et al., 2010; Shinohara et al., 2013); and the function of other proteins (Li et al., 2014).

2.2. Cytoskeleton components and their functions in higher plant cells

The plant cytoskeleton comprises of a widespread complement of filamentous structures designated as microtubules (MT) and actin filaments (AF). Cytoskeleton coordinates such a plethora of biological processes in plants as cell division, cell wall deposition, organelle/vesicle trafficking, cell motility and cell shape maintenance, protection against mechanical stresses and many other (Wasteneys, 2002; Wickstead and Gull, 2011).

MT defines cell growth polarity by the positioning of the multiprotein cellulose synthase complexes at the plasma membrane determining the site of primary cell wall biosynthesis (Paradez et al., 2006; Griffiths et al., 2015), driving cell divisions by the subsequent switch of preprophase bands, mitotic spindles and phragmoplasts and defining the cell division planes (Martinez et al., 2017). In turn, actin cytoskeleton is involved into multiple processes in plant cell such as development, establishment and support of cell polarity, transduction and perception of extra- and intracellular signals including such mechanical stimuli as pathogen penetration due to its dynamicity and rearrangement (Hardham et al., 2008). Plant cell development and various functions are strongly affected by interaction between actin cytoskeleton and endomembrane system (Hussey et al., 2006; Sampathkumar et al., 2013). AF are involved in cell plate formation during cytokinesis and the separation of new daughter cells after the successful segregation of chromosomes into the daughter nuclei (Valster et al., 1997), modulation of stomatal opening in guard cells (Hwang et al., 1997), adjusting cell-to-cell plasmodesmata connections (Aaziz et al., 2001), transduction of gravitropic stimuli in root cells (Braun et al., 2004), “cytoplasmatic streaming” (Schmidt et al., 2007), tip growth of pollen tubes

and root hairs (Schoenaers et al., 2017), regulation of vacuole structure and it's dynamics (Feeney et al., 2013). AF also participate in the response of plant cell to abiotic factors, because they are essential for chloroplast translocation under high light conditions (Suetsugu and Wada, 2012), modulation of amyloplast movement and gravitropic signal transduction (Palmieri and Kiss, 2005), control of protoplast volume during the plasmolytic cycle (Komis et al., 2002), regulation of guard cell volume and the activity of ion channels in the plasma membrane (Hwang and Lee, 2001), selective plant response to electrical fields (Berghofer et al., 2009), and triggering of programmed cell death in pollen tube (Wilkins et al., 2014). These integrated signaling networks undergo structural changes in plant responses to the internal and external cues and play a role of switch of stress tolerance/resistance to various abiotic (photoperiod, mechanical stimuli, temperature changes, etc.) (Nick, 2013) and biotic (infection with viral, bacterial, or fungal pathogens) stresses (Schmelzer, 2002; Takemoto and Hardham, 2004; Kobayashi and Kobayashi, 2007).

2.2.1. Microtubule structure and dynamics

A microtubule is formed by 13 linear protofilaments consisting of head-to-tail assembled α/β-tubulin heterodimers forming homotypic lateral interactions (Nogales, 2015). Commonly multicellular eukaryotic organisms have several α- and β- tubulin isoforms. For instance, *Arabidopsis* genome has 6 highly similar α- and 9 ß-tubulin genes variable at C-terminal end (Kopczak et al., 1992). To form a heterotubulin dimer in *Arabidopsis*, α- and ß-tubulins are required to be co-translated with large chaperone complex from PILZ protein family (Szymanski, 2002). In prokaryotic cells α- and β-tubulin are components of cell division machinery. Thus, procaryotic tubulin homologue FtsZ comprises cytokinetic ring in bacteria and archaea, and TubZ and RepX are important for plasmid division (Chaaban and Brouhard, 2017).

The diversity of the α/β-tubulin complement is further increased via the set of post-translational modifications (PTMs) constituting the so-called tubulin code (Blume at el., 1997; Smertenko et al., 1997; Hammond et al., 2008; Cai 2010; Janke and Magiera, 2020). For instance, plant α-tubulin undergoes reversible tyrosination (Smertenko et al. 1997), tyrosine nitration (Blume et al., 2013), phosphorylation of serine/treonine (Blume et al., 2008) and tyrosine residues (Blume et al., 2010), acetylation (Smertenko et al., 1997), and also polyglutamylation (Cai 2010), methylation (Wloga et al. 2017), while

β-tubulin can be phosphorylated (Blume et al., 2010) and polyglutamylated (Smertenko et al. 1997), as well as nitrated on tyrosine residues (Blume et al., 2013). Tubulin C-terminal end undergoes PTM as cleavage by subtilisin, glutamylation and glycylation of both α- and β-tubulin tails (Wloga et al., 2017).

The diversity of α/β-tubulins at both the transcriptional and the post-translational level has implication in the MT architecture (e.g., Raff et al., 1997) and the MT longevity (reviewed in Janke and Magiera, 2020). MT show elaborate intracellular organization and dynamic behavior which are supported and modulated by diverse accessory proteins associated with them called MT associated proteins (MAPs) (Hussey, 2009). For example, kinesins as one of motor MAPs interact with MT at tracks to transport cargo proteins, and MAP65 are involved in the regulation of MT organization due to their bundling (Krtkova et al., 2016). Domains including γ-tubulin ring complex (γ-TuC), binding/severing/destabilizing proteins adjust cytoskeleton organization and dynamics (Hamada 2007; Horio and Murata 2014; Elliot and Shaw 2018).

In turn, regulation of actin components is largely associated with the huge variety of actin-binding proteins (ABPs) along with bundling proteins, nucleation/ severing factors and barbed-end capping proteins (Blanchoin et al., 2010; Li et al., 2015).

In higher plants during interphase MT are largely concentrated in a cell cortex, while in dividing cells MT are forming appropriate mitotic and cytokinetic arrays (Figure 4).

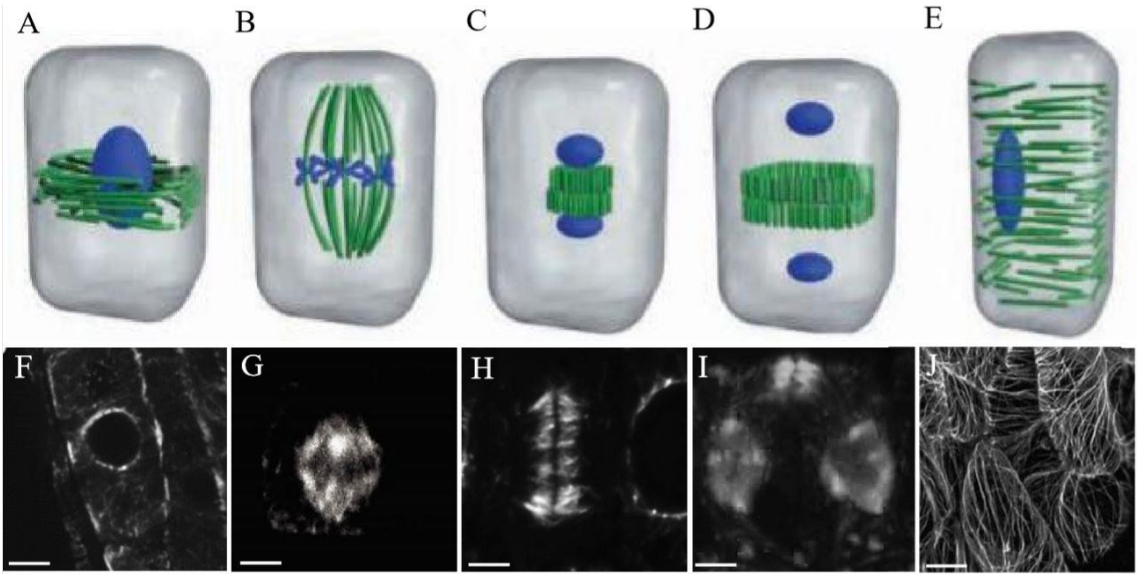

Figure 4. Mitotic and interphase arrays of MT in different stages of plant cell cycle: (A−E) 3D-models (Wasteneys 2002); (F-G) confocal microscopy images. (A) preprophase band; (B) metaphase mitotic spindle; (C) phragmoplast; (D) cytokinetic phragmoplast; (E) interphase

cortical MT; (F) preprophase band in WT in *Arabidopsis* hypocotyl cells of expressing GFP-MBD (Azimzadeh et al., 2008); (G) metaphase mitotic spindle visualized with MAP65-4 in meristematic cells of *Arabidopsis* (Li et al., 2017). (H) phragmoplast in root tip cells of WT (Azimzadeh et al., 2008). (I) cytokinetic phragmoplast in *Arabidopsis* root meristem cells immunostained with anti-tubulin antibody (green) and DAPI-stained nuclei (blue) (Smertenko et al., 2018). (J) interphase cortical MT in WT *Arabidopsis* hypocotyl cells of expressing GFP-MBD (Wasteneys 2002; Azimzadeh et al., 2008). Scale bars: (F) 50 μm; (G,I) 5μm; (H, J) 10 μm.

Mitotic array performs reorganization of cytoplasmatic MT to mitotic spindle, originating with the formation of a pro-spindle and finishing with the metaphase plate (Masoud et al., 2013).

Cortical arrays comprise of individual or bundled MT at the vicinity of the plasma membrane. Their organization is responsive to extrinsic cues and underlies the directionality of cell growth by supporting and guiding the deposition of cellulose microfibrils in the overlying cell wall (Lee and Liu, 2019). As such cortical MT may be randomly distributed during isotropic cell growth, but may assume highly biased configurations, when a preferential growth pattern is induced (Figure 5).

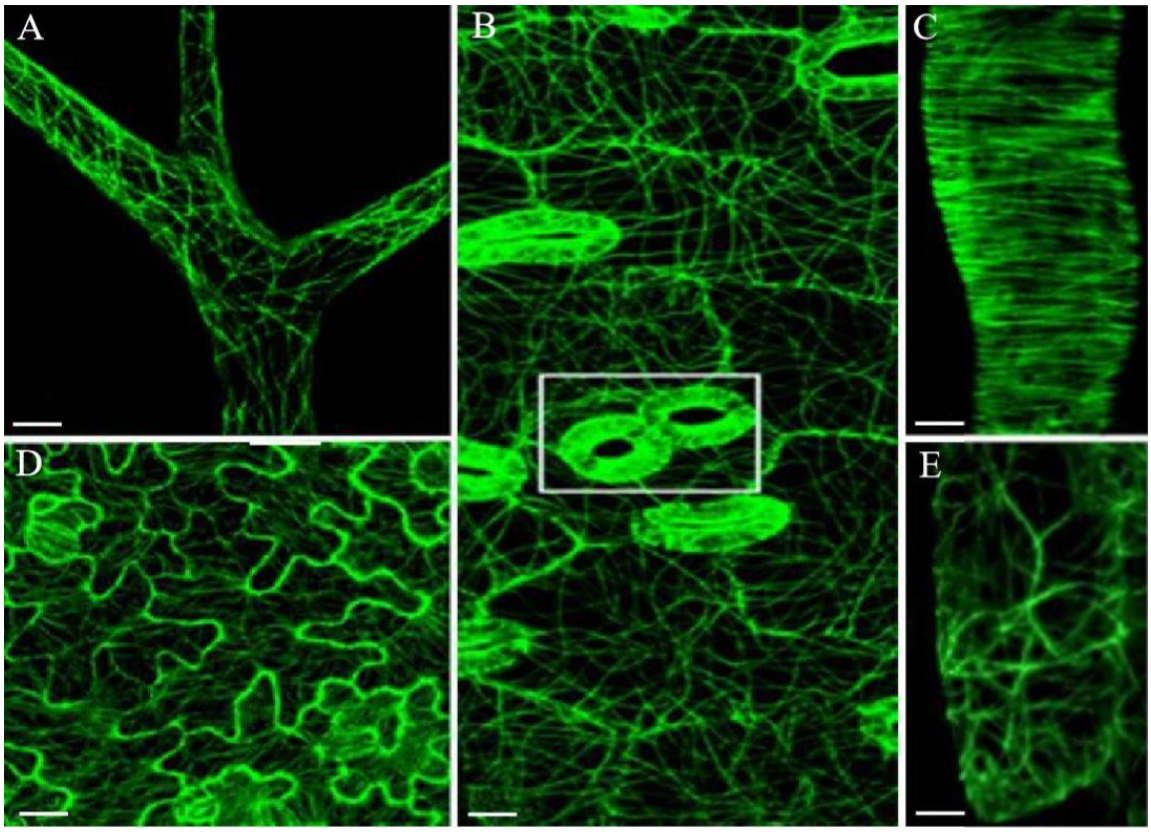

Figure 5. Different arrays of cortical MT in cells of *Arabidopsis thaliana* visualized by an overexpression of different microtubule-binding domains. (A) trichomes, MAP4-GFP; (B) stomata and pavement cells of leaf epidermis, GFP-AtMPB2C; (B) epidermal cells of cotyledons, GFP-TUA6; (C) epidermal cells of elongation zone of primary roots, GFP-TUA6; (E) lateral cells of root cap, MAP4-GFP (Ruggenthaler et al., 2020). Scale bars: (A−D) 40 μm; (C) 10 μm; (E) 5 μm.

MT originate at specific cell sites due to the nucleation process, what involves the rate-limiting formation of a nucleation seed consisting of a few tubulin molecules, which template the further recruitment of αβ-tubulin dimers during MT elongation (Job et al., 2003). Although nucleation may occur spontaneously at permissive concentrations of αβ-tubulin dimers, in cells it is facilitated by a third member of the tubulin family, called γ-tubulin (Desai and Mitchison, 1997). The latter forms ring structures termed γ-tubulin ring complexes (γ-TuRCs), which are accumulated at cellular sites of MT emergence (Desai and Mitchison, 1997).

Both α- and β-tubulins have GTPase activity, hence the αβ-tubulin dimer contains two GTP-binding sites. The GTP-binding site of α-tubulin is considered to be non-exchangeable, and is persistently occupied by GTP, while the GTP-binding site of β-tubulin is potentially exchangeable after stimulation of the GTPase activity of β-tubulin that stochastically occurs during dynamic excursions of the MT. Owing to the inherent polarity of the αβ-tubulin dimer and the head-to-tail fashion of dimer self-associations, the MT itself, is also polarized and exhibits two structurally and functionally different ends. The so-called plus-end which exposes β-tubulin moieties at its tip and the so called minus-end which exposes α-tubulin moieties. As will be seen immediately after, the plus-end is the MT site mostly responsible for MT length fluctuations, while the minus-end is the one associated with γ-TuRCs and exhibits minimal or no dynamic behavior at all (Desai and Mitchison, 1997).

There are two conceptually different dynamic behaviors of MT, namely dynamic instability and treadmilling which either occur individually, or may be combined as it is frequently observed in plant systems (Shaw et al., 2003). Dynamic instability is a mechanism of stochastic alterations between growth and shrinkage that exclusively occurs at the MT plus end. During growth, GTP-bound αβ-tubulin dimers associate at the tip at almost linear rates and promote MT elongation. When for unknown reasons, GTPase activity of the exposed β-tubulin moieties is stimulated, GTP is exchanged for

GDP and the MT starts to rapidly shrink. Shrinkage may continue until the MT is completely depolymerized or may be halted by the addition of GTP-bound αβ-tubulin dimer and the resumption of MT elongation. The stochastic transition from polymerization to depolymerization is called catastrophe while the opposite process is called rescue (Mitchison and Kirschner, 1984; Brouhard and Rice, 2019). During the process of dynamic instability, the minus-end stays indifferent.

On the other hand, treadmilling is a mechanism of MT dynamics involving both MT ends. In the case of treadmilling, tubulin subunits are perpetually lost from the minus end, while other subunits are incorporated at the plus end at roughly the same rate.

MT dynamics is regulated by range of proteins. For instance, orthologues of end-binding-1 protein (EB1) in *Arabidopsis* contributing into MT network organization and bundling (Molines et al., 2018). Moreover, cytoplasmic linker-associated proteins (CLASPs) belonging to MAPs family regulates specific groups of MT, promote mitotic spindle formation and stability and input into MT growth in kinetochores and spindle midzone (Al-Bassam et al., 2010). Furthermore, in *Arabidopsis* SPIRAL1 proteins are involved in the regulation of cortical MT organization during anisotropic cell growth (Nakajima et al., 2006).

Numerous intracellular stimuli and (a)biotic environmental factors induce dynamic adaptive rearrangement of the cytoskeleton (Baluška et al., 2003; Chilley et al., 2006). The orientation of MT and AF along the shoot/root main axis (transverse, oblique, longitudinal, randomized) and their organization (bundled, relaxed, loose, stabilized, fragmented, depolymerized) vary during cell division, elongation, and differentiation. Tissue "growth status," developmental stage, and progress in stress responses are mirrored in MT orientation (Duckett and Lloyd, 1994).

2.2.2. Actin filaments structure and dynamics

Actin filaments comprise of an ubiquitous and evolutionarily conserved protein named actin. Actins consist of three families namely α-, β- and γ- in eukaryotes and bear significant homology with prokaryotic ancestor proteins such as MreB (Schmidt et al., 2007). In cells, actin is distributed between a soluble pool of monomers (G-or globular actin) and a polymer pool consisting of double intertwined filamentous actin chains (F^-actin) as well as many actin-binding proteins for polymerization and severing (profilin, ADF/cofilin, AIP1, CAP, capping protein, CP, formin, villin/gelsolin, α-actinin, fimbrin,

talin, vinculin, etc.) has been implicated in the establishment and maintenance of cell polarity, providing tracks for the movement of assorted cellular organelles, and responses to numerous environmental stimuli (Drobak et al., 2004). Two parallel F-actin strands form microfilaments – higher order structures, which are packed into actin cables, which supposed to be main tracks for organelle intracellular transport (Schmidt et al., 2007) (Figure 6).

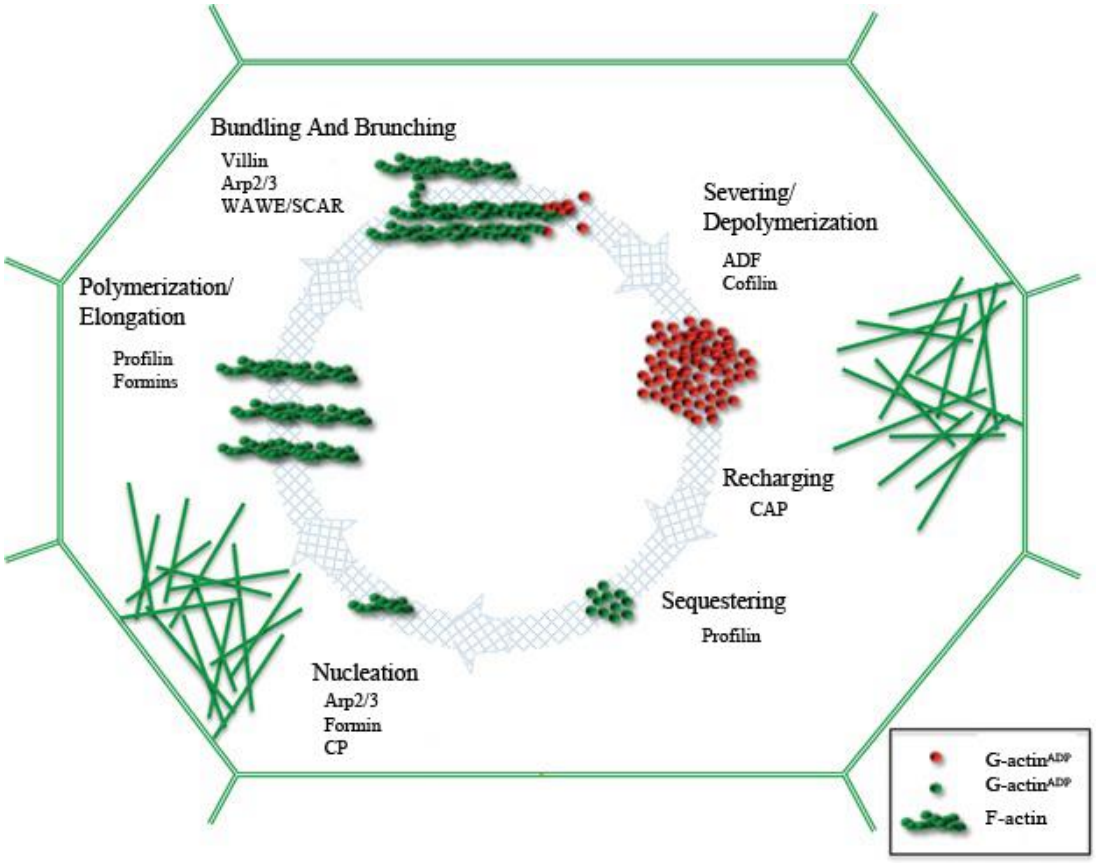

Figure 6. Scheme of actin remodeling in plant cell (Porter and Day 2015).

The nucleation − the multi-step process of AF assambly − is affected by several factors, comprising presence of AF ends, the size of the cellular pool of G-actin monomers, the nucleotide-loaded state of the G-actin monomers and expression of actin-associated proteins (Hussey et al., 2006). The process of nucleation is regulated by multiprotein complex considered as the actin-related 2/3 (Arp2/3) complex (Campellone and Welch, 2010). Additional proteins required for actin nucleation include formin (Chesarone et al., 2010), capping protein (Huang et al., 2003) and gelsolin (Silacci et al., 2004). As nucleation initiation F-actin starts to maturate through filament elongation, that's requires the addition of ^{ATP}G-actin to the plus end of newly nucleated actin-trimmer or to already separated F-actin strand. After the filament becomes mature, ATP hydrolisis,

connected with the actin depolymerzing factor (ADF) proteins, leads to the depolymerization of the filament at the pointed ^{ADP}F-actin end. This process is known as "treadmilling" and it results remodeling of actin under control of amount and direction of F-actin formation (Abeyaratne et al., 2020).

Actin filament network is dynamic structure as a part of cytoskeleton, which performs numerous functions. AF ungergo structural rearrangments in response to inner and outer signals. AF are involved in maintance of cell polarity, organelle traffiking and react to multiple environmental signals (Drobak et al., 2004). Actin network reorganize in response to various abiotic factors like high and low temperature, drought, salt and alkiline stresses (Zhou et al., 2010; Plohovska et al., 2016). It is significant during for the chloroplast movement under higher levels of light (Suetsugu et al., 2010; Suetsugu and Wada, 2012), control of amyloplast alterations and gravitropic signal transduction (Palmieri and Kiss, 2005), adjustment of stomata and the activity of ion channels in plasma membrane (Hawng and Lee, 2001), and induce apoptosis (Thomas et al., 2006; Blume et al., 2017). AF play major role in responses to biotic stress triggered by pathogens (Lu and Day, 2017).

AF's orientation, bundling and density can be evaluated by measuring parameters like mean angular difference, skewness and GFP signal, where skewness is a measure of the degree of asymmetry of a distribution and GFP signal occupancy, which is an indicator of the proportion of pixel numbers constituting the skeletonized MFs of the total pixel numbers constituting the cell region (Higaki et al., 2010).

Actin has a connection with nuclear membrane connection, since SUN (SAD1/UNC84) protein complex is localized in the inner nuclear membrane and interacts with KASH (Klarsicht/Anc/Syne-1 homology) protein (C-tail-anchored membrane proteins, which are targeted specifically to the outer membrane of the nuclear envelope domains at the outer membrane, which associate with actin cytoskeleton (Graumann et al., 2014). Formins are proteins that regulates actin dynamics by functioning at the "barbed end" of the actin filament (Blanchoin and Staiger, 2010).

Moreover, actin cytoskeleton is closely interacting with endoplasmic reticulum (ER), (Sparkes et al., 2011) and Golgi apparatus due to close association of Golgi bodies with ER surface (Sparkes et al., 2009). Recent studies demonstrate that ER seems to be one of the storages of Scar/Wave driving actin polymerization that underlies protrusion of the front of the cell and thus drives migration and the APR2/3 (Actin-Related Proteins)

signaling complexes (Zhang et al., 2013), whose activation promotes AF polymerization and branching.

2.2.3. Regulation of cytoskeleton by phytohormones

Plant hormones are frequently related to cellular events requiring cytoskeletal remodeling. In this context, plant hormones modulate MT and AF orientation/organization, dynamic properties, expression of genes encoding different tubulin/actin isotypes, and their post-translational modifications (Blume et al., 2017).

As other organelles cytoskeleton is affected by different types of phytohormones. For instance, auxins enhance number of cells with transverse MT organization essential for root growth and differentiation (Baluška et al., 1996; Takesue and Shibaoka, 1999), playing the major role in cortical MT reorientation (Takesue and Shibaoka, 1999), depolymerization (Blancaflor et al., 1995) or reassembly (Baluška et al., 1996). Auxins causes dissociation of actin bundles into individual filaments (Wang and Nick, 1998) and reduce the length of elongation zone in primary roots of *Arabidopsis* via enhanced formation of actin budles (Rahman et al., 2007). Next, cytokinins causes increasing of cytosolic Ca^{2+} amount due to its release from the intracellular storage sites that may result in the increased tension of transvacuolar microfilament network (Grabski and Schindler 1996). Moreover, cytoskeleton is participant in plant symbiotic interactions such as formation of arbuscular mycorrhiza and nodulation, which requires high levels of cytokinins (Murray et al., 2011).

Abscisic acid (ABA) increases MT stability during low temperature stress (Nick, 2008). MT depolymerization provides higher amount of stable MT after ABA treatment, which results declaration of plant development on the first steps of cold acclimation. After cold acclimation plant MT polymerization increase, providing more dynamic unstable MT (Timofeeva et al, 2000). ABA affects stomatal movement through reorganization of microfilaments in the cell from radial to randomized and fragmentated. Rapidly after ABA treatment in stomatal cells occurs microfilament decomposition, leading to their closure and effect progresses with time (Eun et al., 2001). Ethylene treatment provided longitudinal or oblique orientation of MT (Roberts et al, 1985).

Jasmonic acid (JA) and its derivate methyl jasmonate (MeJA) are essential components for plant's responses to stresses caused by ozonation, injuries enhanced contact with UV light and protection again patogens (Schmidt and Panstruga, 2007; Janda

et al., 2014). The pathogen invasion into plant cell produce signal to enhance JA synthesis, which affects cytoskeleton reorganization to create barrier against infection by activation of callose synthesis (Hardham et al., 2007; Blume et al., 2017).

Salicylic acid (SA) and its derivate methyl salicylate (MeSA) maintain vital role as signaling molecules during heat, cold, ozonation, biotic and ROS stresses. Damage of actin cytoskeleton trigger SA to induce expression of PR (PATHOGENESIS-RELATED) proteins as a response to pathogen invasion (Matoušková et al., 2014; Blume et al., 2017).

2.3. Strigolactones and cytoskeleton

SL and ethylene share common signaling pathways in the control of root hair formation, where ethylene is epistatic to SL, whereas the effect of SL on root hair elongation requires ethylene synthesis (Kapulnik et al., 2011). Moreover, SL are probably regulators of auxin flux, since they can repress bud outgrowth locally and/or indirectly by affecting PIN-mediated polar auxin transport in the primary root provascular tissue (Koltai, 2014). Treatment with the synthetic strigolactone GR24 resulted in the reduced fluorescence of GFP-fused auxin transporters PIN1, PIN3, and PIN7 (Koltai, 2011). A model of SL signaling in the root combines both cellular reception and non-cell-autonomous signal transduction. Following cellular reception of SL via the D14-like/MAX2-like/SCF–E2 module, certain receptors are degraded. This leads to the release of downstream targets, and eventually to changes in actin bundling. Reduced or increased actin bundling enhances or reduces the trafficking of PIN proteins, and thereby increases or reduces their polarity in the plasma membrane, respectively. These changes in the cytoskeleton and PIN1 localization might happen in the same cell that perceives the SL signal, or in adjacent cells, via additional signal transduction. The polar position of PINs in the plasma membrane is an important determinant of the direction of auxin flux; therefore, these SL-induced changes in PIN localization may lead to changes in auxin flux. Because auxin modulates actin organization and enhances PIN polarization, the signal from SL for auxin transport may lead to a regulatory circuit of auxin and its own transport (Koltai, 2014). Furthermore, proteomic analysis of GR24-responsive rice proteins revealed differential expression of important enzymes of the carbohydrate/amino acid metabolic pathways and key components of the cellular energy generation machinery (Chen et al., 2014). It was also found that SL (using GR24, a synthetic, biologically active SL analogue) affect auxin efflux transporter PIN2 polar localization, increase PIN2

endosomal trafficking, actin de-bundling, and actin dynamics in a MAX2-dependent fashion in *Arabidopsis* trafficking (*tir3*), actin (*der1*), and PIN2 (*eir1*) mutants (Pandya-Kumar et al., 2014). GR24 increased polar localization of PIN2 in the PMof epidermal cells and accumulation of PIN2-containing brefeldin A (BFA) bodies, increased ARA7-labeled endosomal trafficking, reduced F-actin bundling, and enhanced actin dynamics, all in a MAX2-dependent manner. Most of the *der1* and *tir3* mutant lines also displayed reduced sensitivity to GR24 with respect to root hair elongation (Pandya-Kumar et al., 2014). Treatment of WT TALIN-GFP and FABD2-GFP expressing seedlings with GR24 caused the reduction in actin filament bundling in the epidermal cells of the root tip elongation zone evidenced by an increased proportion of thin fibrils and a decreased proportion of thick fibrils with the significant reduction in skewness. Unlike the WT, however, application of GR24 to *max2*-1 mutant expressing TALIN-GFP under the 35S promoter did not reduce actin filament bundling. Together, the results suggest that bundling of actin filaments in the epidermal cells of the primary root elongation zone is reduced upon GR24 treatment in a MAX2-dependent fashion. GR24 treatment seems to reduce F-actin bundling in the epidermal cells of the primary root elongation zone, which in turn would enhance actin destabilization and thus actin susceptibility to depolymerization by the actin-depolymerizing substance latrunculin B (Pandya-Kumar et al., 2014). Besides that, SL affect actin dynamics in the WT but not in *max2-1* at GR24 plates, since the increased F-actin average and median velocity in the epidermal cells of the root tip elongation zone was detected.

Concerning MT, SL analogues MEB55 and ST362 compromise the integrity of the MT network and may inhibit the migratory phenotype of the highly invasive breast cancer cells (Mayzlish-Gati et al., 2015). Moreover, SL analogues activate apoptotic p38 (mitogen-activated protein kinase) cascade and inhibit cyclin B expression (Pollock et al., 2014). However, there are no reports on SL effects on plant MT so far.

3. MATERIALS AND METHODS

3.1. Plant material

Wild-type (WT *A. thaliana* (Columbia-0), SL-insensitive T-DNA insertion *A. thaliana* mutant *max2-1* (*more axillary growth*) (EMS mutant; Stirnberg et al., 2002) on Col-0 background kindly provided by Prof. H. Koltai were used in this study. MT organization

was recorded in *A. thaliana* Col-0 wild type or *max2-1* mutant seedlings stably expressing a *35S::GFP-MBD* (microtubule binding domain of mammalian non-neuronal MAP4 microtubule associated protein), or a *35S::TUA6-GFP* construct (Marc et al., 1998; Shaw et al., 2003). Actin microfilament organization was documented in *Arabidopsis* seedlings transformed with the *35S::Lifeact-GFP* construct (LifeAct includes the first 17 amino acid from the *Saccharomyces cerevisiae* Abp140, an actin-binding protein; Riedl et al., 2008). Actin organization was also documented in *Arabidopsis* lines bearing the GFP-fABD2 actin marker (Voigt et al., 2005). *max2-1* mutants were crossed with Col-0 wild type transformed with *35S::GFP-MBD* or *35S::TUA6:GFP* constructs. To ensure a homozygous background of the crossed lines we used the T3 generation. All seedlings expressing microtubule or actin markers were selected under epifluorescence microscope and used thereon for documentations with either the CLSM or the spinning disc microscopes.

3.1.1. Seed sterilization

Seeds of transformed or untransformed Col-0 or *max2-1* were surface sterilized with 1% v/v sodium hypochlorite (NaClO) solution supplemented with a drop of 0.1% v/v Tween-20 as a surfactant for 10 min, short-spin vortexed, immersed to 70% v/v ethanol for 5 s, thoroughly rinsed 5 times by sterile MilliQ water and placed to square Petri dishes containing 0.6% w/v agarose-solidified ½ Murashige and Skoog medium (½ MS; Duchefa) with 1% w/v sucrose with or without exogenous synthetic SL and/or inhibitors of endogenous SL biosynthesis. All manipulations with seeds were carried out in aseptic conditions in laminar flowbox using instruments immediately sterilized in 70% v/v aqueous ethanol or Spitaderm disinfectant solution (e.g., tweezers) or wooden toothpicks autoclaved before use. Solution exchange was performed with the use of an automatic Eppendorf micropipette.

3.1.2. Culture medium preparation and sowing

Arabidopsis seedlings were cultivated on solid ½ MS medium containing 10 g of sucrose, 1 g of MES buffer, 2,15g of basal MS salts and 6 g of agarose or Gellan gum for 1 L of Milli Q water. KOH (1M) was used to adjust pH at 5.8. After that freshly prepared

medium was autoclaved at 121°C for 20 min. Thermoindicative tape was used to prove that the sterilization conditions were sufficient.

Thereafter, the sterile medium was poured into square Petri dishes (120 mm × 120 mm) in a sterile laminar flowbox with further sealing with parafilm after solidifying. Circa 30 seeds were sown on each dish by using micropipette with tips slightly cut at the end (5−10 µl). After seeds sowing Petri dishes were covered with parafilm (still in sterile flowbox) to prevent bacterial or fungal contaminations.

3.1.3. Growth conditions

Petri dishes with seeds were stored for 1 d at 4°C to synchronize germination and then germinated at a vertical position in Phytotron at 22°C under long-day conditions (16 h light/8 h darkness, PPF: 150 µmol m−2 s−1) for 4 or 7 d prior to imaging. To promote etiolation, Petri dishes were wrapped in aluminum foil after seeding, stratified and germinated as such under the same environmental conditions.

3.2. Chemicals and laboratory devices

3.2.1. Commercially available chemicals

Unless stated otherwise, all common chemicals were from Sigma and were of analytical grade. . In turn, GR24 was synthetized by Tomáš Pospíšil or purchased from Chiralix (Nether lands), while TIS108, a triazole-type strigolactone biosynthesis inhibitor was purchased from Chiralix (Netherlands).

3.2.2. Laboratory devices and materials

Analytical balances (XA 110/2X, RADWAG, Waga Elektronicze)
Electromagnetic stirrer IKA Combimag REO (Drehzahl Electronic)
Flowbox biohazard (Faster)
ImageScanner™ III (GE Healthcare)
Laboratory fridge (Electrolux, Space Plus, ERB 34633W)
Laboratory hood (M1200, MERCI)
pH meter (TEMP RS232, PL-600 pH/mV/Temp Meter, EZODO)
Phytotron (WEISS Gallenkamp)

Precision balances (S1502, BEL-Engineering)
Simplicity water purification system (Millipore)
Eppendorf microtubes (1,5 ml; 2 ml) beakers, volumetric cylinders, tweezers, wooden toothpicks, filter paper, magnetic stirrers, sterile tips, scissors, sterile square Petri dishes (25 and 40 ml), borosilicate glass slides, coverslips (20x20 mm, 32x64 mm), Parafilm stripes, liquid petroleum jelly (nail polish), double-sided sticky tape, Zeiss Immersion Oil 518F

3.2.3. Microscopes

Stereo microscope (MSZ5000, A. Krüss)
Axio Zoom.V16 (Carl Zeiss, Germany)
Epifluorescence microscope (Axio Imager M2, Carl Zeiss, Germany)
Confocal microscope (LSM 710, Axio Imager Z2, Carl Zeiss, Germany)
Spinning-disk microscope (Cell Observer Z.1; Carl Zeiss, Germany)

3.3. Chemical treatment

A synthetic specific SL *cis*-GR24 consisting only of D14-perceived GR24+ synthesized by Tomáš Pospíšil according to Zwannenberg et al., 2013) was dissolved *ex tempore* in pure anhydrous acetone to prepare a 10 mM stock solution from which, working concentrations of 1, 3, 10 and 25 μM were prepared. 4-d-old seedlings were taken from 0.6% w/v agarose-solidified media, treated with GR24 and prepared for microscopy. A triazole-type SL biosynthesis inhibitor designated as TIS 108 (Chiralix, Netherlands) was dissolved in pure, anhydrous acetone prior to use to have 10 mM stock solution further diluted to 3 and 10 μM final concentrations and added to agarose-solidified ½ MS medium or used for short-time treatment in liquid MS.

3.4. Crossings of Arabidopsis *max2-1* mutants with plants stably expressing 35S::GFP-MBD and 35S::GFP-TUA6 constructs

To track changes in microtubule organization in cells of *Arabidopsis* hypocotyl under GR24 and TIS108 treatment 4-weeks-old *max2-1* plants (acceptor, “mother”) growing in circular pots were pollinated with pollen and MAP4-GFP- of TUA6-GFP- bearing plants (donors, “fathers”). For crosses we have chosen undisclosed flowers of *max2-1* mutant to

prevent self-pollination. Pollen was taken from mature flowers of donor plants (Figure 7, A–C).

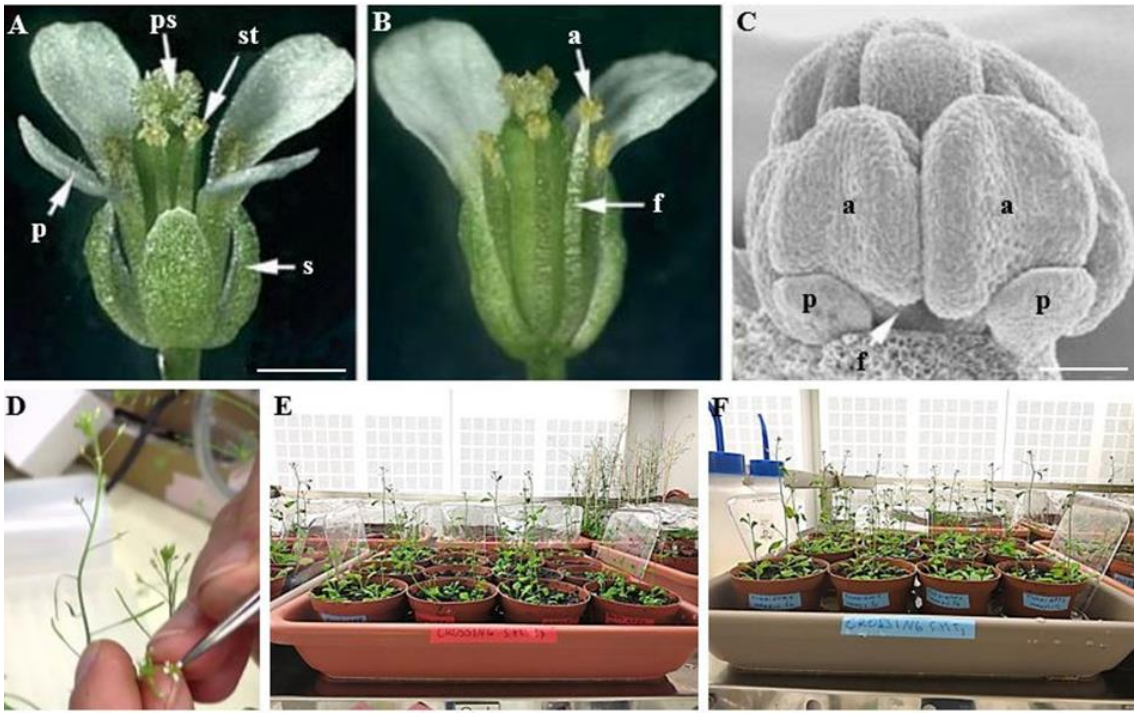

Figure 7. Crossing of *Arabidopsis* plants: (A) an intact mature flower with sepals (s), petals (p), stamens (st), and the pistil (ps); (B) a mature flower with the exposed stamens having an anther (a) and a filament (f). Scale bar: 1 mm; (C) a scanning electron micrograph showing inner structure with two petal primordia (p), anthers (a) with the characteristic lobed shape and the very short filament (f). Scale bar: 100 μm. Images A–C are adapted from Ma (2005). (D) choosing stamen bearing pollen with a tweezer (from the video tutorial: https://www.youtube.com/watch?v=QVIPBEwBG5k); (E,F): 1-week-old crosses of T3 generation of both *max2-1*:MAP4-GFP and *max2-1*:TUA6-GFP growing in standard light/dark conditions in phytotron.

Undisclosed flowers of *max2-1* were slightly opened with pizzetta and pollen from the 2-3 separated stamens of *Arabidopsis* (MAP4-GFP) or (TUA6-GFP) was gently transposed inside the mother plant flowers either under the control of a binocular/magnifying glass, or with a naked eye (Figure 7, D). Generally, on each mother plant not more than 2-3 flowers were pollinated in order not to traumatize it too much. Pollinated plants were marked with red threads and left in mini-green house constructed from square Petri dishes coiled with cling film for keeping the soil wet for a week before

unwrapping (Figure 7, E,F). All plants were grown in a phytotron at 16h/light and 8h/dark at 25 °C and were regularly watered.

The process was repeated for T2 and T3 generation. Crossings for T3 were *max2-1*:MAP4-GFP and *max2-1*:TUA6-GFP. Seeds for the next generation were harvested from 8- to 10-week-old plants, which were covered with paper bags firmly attached to their stems. Plants were allowed to dry at room temperature (25°C) prior to seed collection.

3.5. Hypocotyl growth rate and phenotypical analysis

Petri dishes with germinated light-grown or etiolated seedlings of Col-0 wild type or *max2-1* mutant at 7^{th}–10^{th} days after germination were placed in scanner (Image Scanner III, EpsonScan) and scanned at transmitted light mode in order to document and subsequently quantify hypocotyl length.

For hypocotyl width measurements, such grown Col-0 wild type or *max2-1* seedlings were documented with differential interference contrast of a widefield microscope (Axio Imager M2, Carl Zeiss, Germany) equipped with a polarizer and a Wollaston prism at three distinct parts of the hypocotyl: the upper part – situated right beneath the cotyledon petiole; the middle part – at the mid-plane of hypocotyl, and the lower part – at the border with the primary root.

For the detailed morphological studies seedlings at 4^{th} and 7^{th} days after germination were documented using Axio Zoom.V16 Stereo Zoom system (Carl Zeiss, Germany) in bright field illumination (objective lenses PlanApo Z 1.5x, FWD = 30mm), and processed in Image J software in Fiji macros (an open platform for scientific image analysis https://imagej.net/Downloads). Hypocotyl length (circa n=30 for each treatment, three repetitions) is presented as mean±SE. All graphical plots were prepared in Microsoft Excel software.

3.6. Microscopy

For live documentation of microtubules and actin microfilaments in Col-0 wild type or *max2-1* mutants expressing proper fluorescent markers we used an LSM710 spectral

CLSM and a Cell Observer spinning disc platform according to previously published specifications (Komis et al., 2014; 2015).

4-d-old seedlings grown at solidified mock, GR24- or TIS108-containing media were mounted between a microscope slide and a coverslip in 30 μL of liquid ½MS medium spaced by double-sided sticky tape, narrow Parafilm stripes and extra sealed using liquid petroleum jelly (nail polish) to form a chamber prior to imaging for sample stabilization. This prevented dislocation of the plantlets during liquid exchange and allowed the observation of the same area during 2 h. All preparations involving etiolated seedlings were done in dark room under dim red or green light.

The GFP-MBD marker was used to extrapolate microtubule organization by means of CLSM, using a 63×1.40 Plan-Apochromat oil immersion objective (1.4 NA) with a 488 nm excitation line, and detection of the GFP signal at 510/540 nm. Laser power was set to no more than 2% of the total output available. Z-stacks were acquired using a 0.61 μm step size.

To document actin organization we took into account the fast dynamics of cortical actin microfilaments which prohibited the acquisition of z-stacks via CLSM. For this reason spinning microscopy was used instead using a Cell Observer Z.1 platform (Carl Zeiss, Germany). Acquisitions were done with a 63×/1.4 NA oil immersion objective. For excitation of GFP a 488-nm excitation laser line was used, while the signal was detected with a BP525/50 emission filter. Images were recorded with a high-resolution Evolve 512 back-thinned EM-CCD camera (Photometrics) with the exposure time 500–750 ms per optical section.

3.7. Analysis of microtubule organization

The organizational patterns of cortical microtubules of Col-0 or *max2-1* seedlings expressing the GFP-MBD marker and treated or untreated with GR24 or TIS108, was analyzed by applying the Cytospectre freeware on full CLSM frames of hypocotyl cells (Kartasalo et al., 2015). In this way, we acquired a semi-quantitative overview of cortical microtubule angular distribution. Briefly, appropriate Z-stacks of hypocotyl cells were summed-up to maximum intensity projections, exported as tiff files and subsequently loaded to the software.

3.8. Quantitative analysis of actin filament organization

Cortical actin microfilament organization was documented in maximum intensity projections after spinning disc imaging of Col-0 or *max2-1* seedlings expressing the GFP-Lifeact marker and treated or untreated with GR24 or TIS108. In all cases, two features were quantified. Average fluorescence per unit area (occupancy; signifying the extent of actin filament bulk) and skewness of fluorescence distribution (denoting the extend of actin filament coalescence and bundling). Both measures, were deduced from values in the Histogram add-on of Zeiss Zen software (licensed Blue version).

3.9. Statistics

Statistical analysis datasets presented herein was performed in the software STATISTICA (version 13.4.0.14; Statsoft, USA) and were contributed by Mgr. Tereza Vavrdová. For comparing two different experimental conditions (light-dark and inhibitor treatment), two-way ANOVA followed by Scheffé's test was used. For pairwise comparisons, one-way ANOVA was used.

4. RESULTS

In the present thesis we focused on the responses of plant microtubules and actin filaments to the fluctuations of strigolactone levels, regulated both pharmacologically (by exogenous GR24 application or by biosynthetic inhibition with TIS108) and genetically (by using the strigolactone-insensitive mutant *max2-1*). Previously published results show that strigolactones as a new class of phytohormones together with “classical” ones such as auxins, cytokinins, gibberellins and abscisic acid, orchestrate morphogenesis and growth of aboveground plant parts. Since such hormones exert developmental roles in part via the indirect regulation of microtubules and actin filaments (Blume et al., 2017) we examine such possibilities in the case of strigolactones during hypocotyl growth inhibition.

Previously, it was reported that strigolactones change architecture and dynamics of actin filaments in *Arabidopsis* root cells (Pandya-Kumar et al., 2014). Namely, GR24 reduces F-actin filament bundling in a MAX2-dependent manner and, at the same time,

enhances actin dynamics, affects endosome trafficking and PIN2 localization in the plasma membrane (Pandya-Kumar et al., 2014).

As for the effects of strigolactones on plant microtubules, there are no reports up to date. However, in the highly invasive breast cancer cells, potent strigolactone analogues MEB55 and ST362 disrupt microtubular networks and alter the cell phenotype (Mayzlish-Gati et al., 2015).

Therefore, our studies were aimed to fill this gap and get data showing the regulation of plant cytoskeleton by strigolactones as it was done for other phytohormones. First of all, we addressed the GR24- and TIS108-induced changes of light-exposed and etiolated hypocotyl length and width of both wild type Col-0 and strigolactone-insensitive *Arabidopsis* mutant *max2-1* using ZOOM stereomicroscopy (phenotypic analysis). Next, the putative changes of cortical microtubules network organization were studied with the help of CLSM. For this reason, we performed crosses and get two mutants, *max2-1*:MAP4-GFP and *max2-1*:TUA6-GFP (T3), stably expressing GFP-reporter constructs. In turn, the organization of actin filaments and the presence of acquosomes was documented with spinning disk microscopy.

4.1. Phenotype characterization

4.1.1. Hypocotyl length and width of light-exposed *Arabidopsis* WT and max2-1 mutant seedlings

To analyze the inhibition of hypocotyl growth and epidermal cell swelling induced by strigolactones, we used 7-day-old WT and *max2-1* mutant seedlings growing on ½ MS medium supplemented with different concentrations of GR24 or TIS108, either in the standard light/dark regime of the phytotron or under conditions of continuous darkness to promote etiolation. It is noteworthy that we have tested from the very beginning a wide range of GR24 concentrations (namely, 0.5, 1, 3, 10, 25 and 50 μM) to finally narrow this range between 3 μM and 25 μM. Moreover, we examined three concentrations of TIS108 (3, 5 and 10 μM) and have chosen the first option as both physiologically relevant and efficient. Seedlings growing in Petri dishes were scanned and images were processed by ImageJ (Fiji 1.46r.) software. Both WT and mutant were represented by at least thirty seedlings. The data were processed in MS Excel 2016 whereby all the charts were created.

For this experiment we used standard light/dark regime of the phytotron or etiolation (Petri dishes with plated seeds were wrapped with aluminum foil) and cultivated WT and *max2-1* mutant seedlings on ½ MS medium containing 3 µM and 25 µM GR24 or 3 µM TIS108. Under the light/dark regime GR24 inhibited hypocotyl elongation and induced mild radial swelling of epidermal hypocotyl cells by comparison to mock-treated Col-0 seedlings (Figure 8A,I cf. Figure 8B,C,J,K).

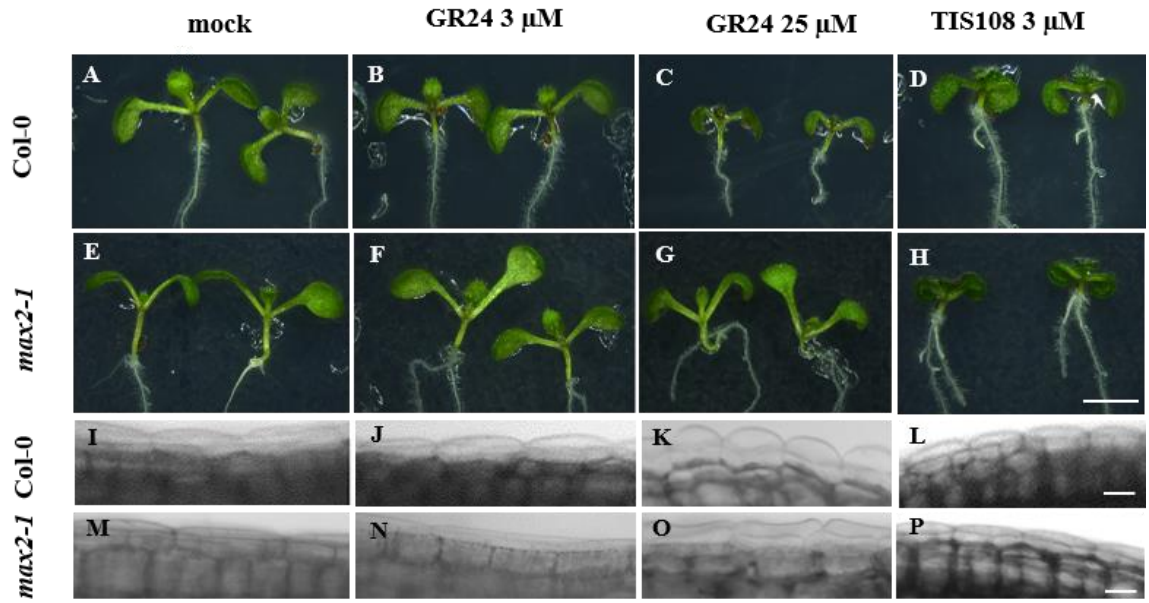

Figure 8. Hypocotyl growth of *Arabidopsis thaliana* Col-0 WT or *max2-1* mutant in the presence or absence GR24 (3 and 25 µM) or TIS108 (3 µM) under standard light/dark regime. (A-D) Hypocotyls of Col-0 seedlings treated with acetone (mock; A), 3 µM GR24 (B), 25 µM GR24 (C), and 3 µM TIS108 (D). (E-H) Hypocotyls of *max2-1* mutant seedlings treated with mock (E), 3 µM GR24 (F), 25 µM GR24 (G), and 3 µM TIS108 (H). (I-L) Detailed widefield documentation of hypocotyl epidermal cells of Col-0 treated with solvent alone (mock; I), 3 µM GR24 (J), 25 µM GR24 (K), and 3 µM TIS108 (L) showing mild cell swelling in all treatments (J-L) as compared to control (I). (M-P). Detailed widefield documentation of hypocotyl epidermal cells of *max2-1* hypocotyl epidermal cells treated with solvent alone (mock; M), 3 µM GR24 (N), 25 µM GR24 (O), and 3 µM TIS108 (P). Scale bars: 5 mm (A-H); 5 µm (I-P).

The SL biosynthesis inhibitor TIS108 caused evident hypocotyl growth inhibition as well (Figure 8D,L). With appropriate measurements it was found that the average hypocotyl length of mock-treated Col-0 seedlings was 2.05±0.145 mm (mean±SD; Figure 9A; N=75).

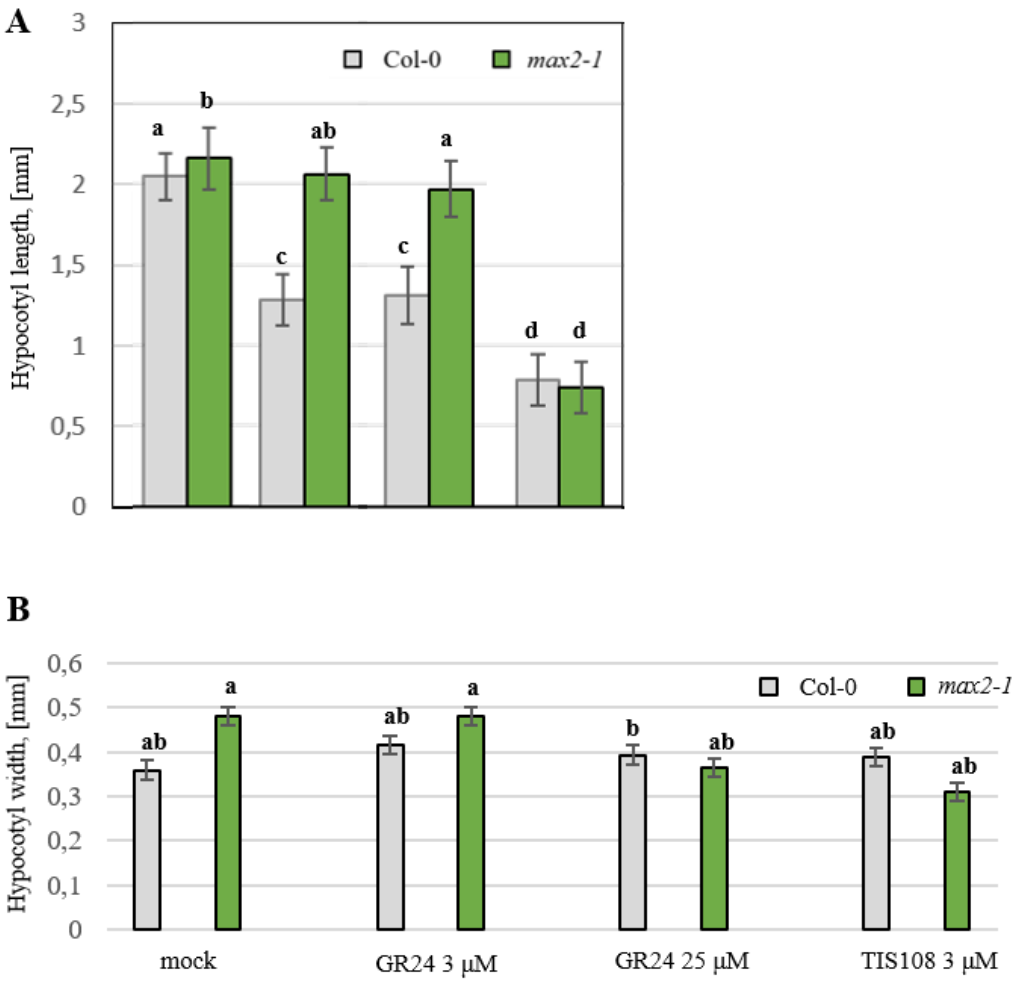

Figure 9. (A). Pairwise comparison of hypocotyl length of Col-0 and *max2-1* seedlings grown under standard light conditions and treated with mock, 3 µM of GR24, 25 µM of GR24 and 3 µM of TIS108. Statistical evaluation was done by two-way ANOVA, followed by Scheffé's post hoc test (N≥59; same letters in the graph indicate groups without statistically significant differences at the 0.001 probability level). (B). Pairwise comparison of hypocotyl width of Col-0 and *max2-1* seedlings grown under standard light conditions and treated with mock, 3 µM of GR24, 25 µM of GR24 and 3 µM of TIS108. Statistical evaluation was done by two-way ANOVA, followed by Scheffé's post hoc test (N≥27; same letters in the graph indicate groups without statistically significant differences at the 0.001 probability level).

After 3 µM GR24 treatment, hypocotyls were shorter and their average length was 1.28±0.158 mm (mean±SD; Figure 9A; p=0.0000; N=60). Treatment with 25 µM GR24 was different compared to mock but was not significantly different to that with 3 µM GR24 and the hypocotyl length in this case was 1.307±0.178 (mean±SD; Figure 9A;

N=56; p=0.0000 and p=0.9992, respectively). Treatment with 3 μM TIS108 resulted in severe hypocotyl growth inhibition, showing average length of 0.783±0.160 mm (mean±SD; Figure 9A; N=61). This treatment was the most diversified from all other conditions being significantly different from all of them (p=0.0000 and p=0.0000 as compared to 3 μM GR24 treatment, and p=0.0000 as compared to 25 μM GR24 treatment).

Using epifluorescent microscopy we addressed also hypocotyl width. It has to be mentioned that the samples were prepared extremely carefully not to squeeze them under the coverslip and prevent extra damage of the swollen cells after some treatments. It was found that the hypocotyl width was only mildly affected by any of the treatments used herein. The width of control Col-0 hypocotyls was 0.309±0.04 mm (mean±SD; Fig. 9B; N=58), 0.325±0.07 mm after 3 μM GR24 treatment (mean±SD; Figure 9B; N=89), 0.290±0.08 mm − after 25 μM GR24 (mean±SD; Figure 9B; N=90), and 0.323±0.05 mm after 3 μM TIS108.

In addition to hypocotyl growth studies of the WT, hypocotyl length and width of *max2-1* mutants grown under the light/dark regime were measured as well. In mock-treated mutants (Figure 8E) but also after treatment with both 3 μM (Figure 8F) and 25 μM GR24 (Figure 8G), the hypocotyl was consistently longer when compared to Col-0 seedlings. The hypocotyl length of *max2-1* mutant seedlings was only affected by 3 μM TIS108 (Figure 8H). Meanwhile, hypocotyl epidermal cells of max2-1 do not show any noticeable changes at any treatment used (Figure 8M-P). In quantitative terms, the hypocotyl length of mock-treated *max2-1* mutants was 2.16±0.19 mm (mean±SD; N=78), 2.06±0.17 mm after treatment with 3 μM GR24 (mean±SD; N=69), 1.98±0.17 mm − 25 μM GR24 (mean±SD; N=80) and 0.74±0.16 mm − 3 μM TIS108 (mean±SD; N=59).

4.1.2. Hypocotyl length of etiolated *Arabidopsis* WT and *max2-1* mutant seedlings

Several publications are dedicated to a synergy between exogenous application of strigolactones and the illumination conditions during seedling growth (e.g., Xie et al., 2020). Therefore, treatments with GR24 (3 μM and 25 μM) and TIS108 (3 μM) were repeated with Col-0 and *max2-1* seedlings grown under continuous darkness. Hypocotyl length of etiolated Col-0 seedlings (Figure 10) exceeded that of light-grown ones (Figure 9A).

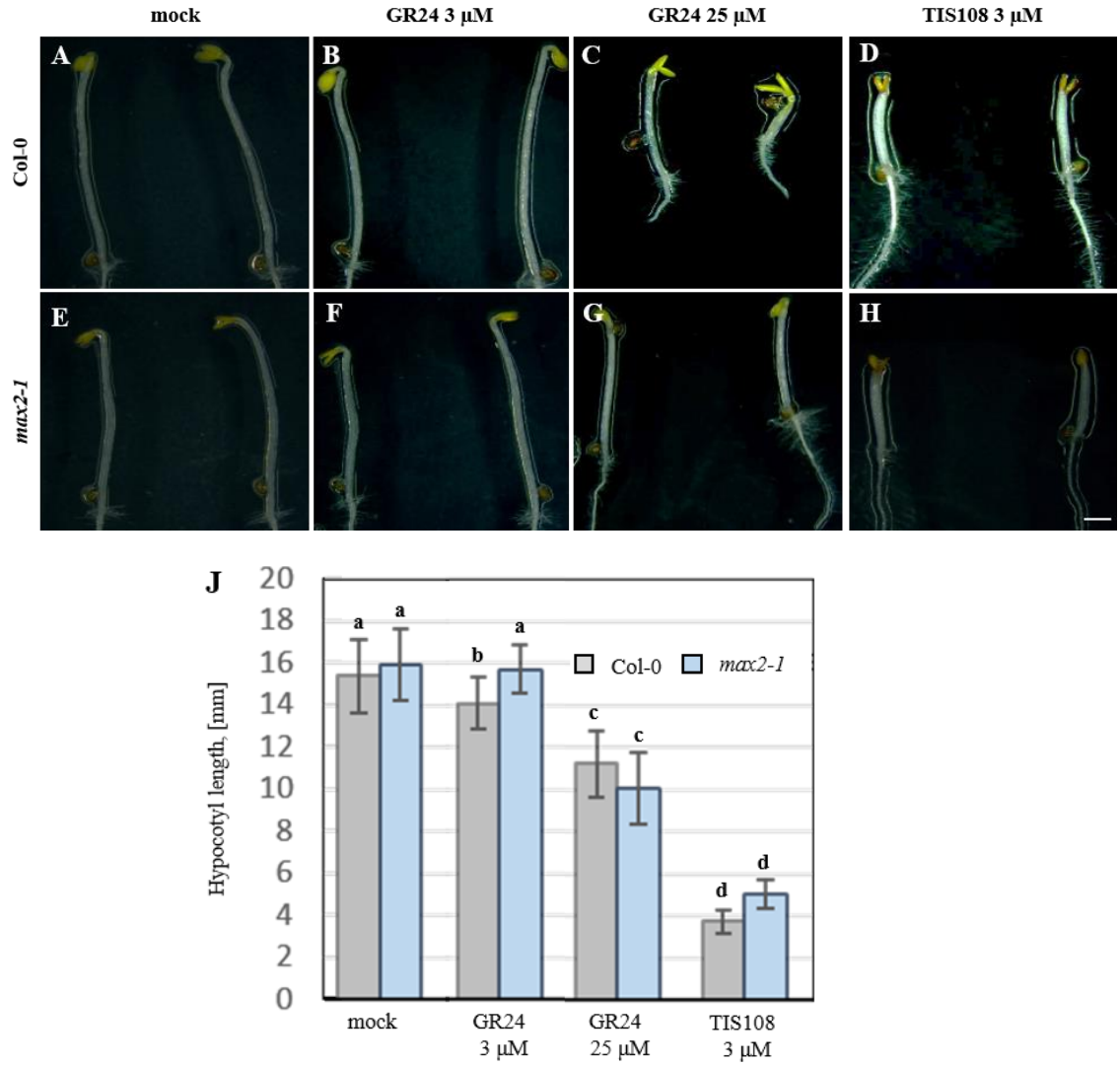

Figure 10. Elongation of hypocotyl in etiolated *Arabidopsis thaliana* Col-0 wild type and *max2-1* mutant seedlings, before or after treatment with GR24 (3 µM and 25 µM) or TIS108 (3 µM). (A−E). Etiolated hypocotyls of mock-treated Col-0 (A), or following treatment with 3 µM of GR24 (B), 25 µM of GR24 (C,D), and 3 µM of TIS108 (D). (E-H) Appearance of etiolated *max2-1* mutant seedlings in the presence of solvent alone (mock; E), 3 µM of GR24 (F), 25 µM of GR24 (G), and 3 µM of TIS108 (H). (I). Quantification of etiolated Col-0 and *max2-1* hypocotyl length after treatment with mock, 3 µM of GR24, 25 µM of GR24 and 3 µM of TIS108 (N≥22; two-way ANOVA with Scheffé's post-hoc test; common letters denote groups without statistically significant differences at the 0.001 probability level). Scale bars: 10 mm (A-H).

Visual documentation and quantitative analysis, showed that etiolated Col-0 seedlings were affected by treatments with 3 µM (Figure 10 B,J) and 25 µM GR24 (Figure 10C,D,J), but they proved most responsive to 3 µM TIS108 (Figure 10 E,J). The length of control etiolated Col-0 seedlings was 15.45±1.77 mm (mean±SE; N=78), 14.09±1.22

mm after treatment with 3 μM GR24 (mean±SE; N=75), 11.23±1.54 mm after treatment with 25 μM GR24 (mean±SE; N=77) and 3.74±0.56 mm after treatment with 3 μM TIS108 (N=36). By statistical deductions, all treatments significantly reduced the hypocotyl length of etiolated seedlings when compared to the mock treatment (Figure 2J; p=0.0000 for 3 μM of GR24; p=0.0000 for 25 μM of GR24; p=0.0000 for 3 μM of TIS108). These treatments were repeated on the *max2-1* mutant (Fig. 10F-I), which was also sensitive to both GR24, and to TIS108. Compared to mock-treated *max2-1* seedlings (Figure 10F), which exhibited length of 15.95187 ±1.64 mm (mean±SD; N=23), those treated with 3 μM GR24 (Figure 10 G) were 15.72±1.12 mm (188 mean±SD; N=30), with 25 μM GR24 (Fig. 10 H) − 10.05±1.66 mm (mean±SD; N=22), and 3 μM of TIS108 (Fig. 2I) − 5.06±0.64 mm (mean±SD; N=25) long. Most treatments conferred significant changes on hypocotyl length of etiolated *max2-1* seedlings compared to controls with the exception of 3 μM GR24 (Figure 10 J; p=0.9998 for 3 μM GR24; p=0.0000 for 25 μM GR24; p=0.0000 for 3 μM TIS108).

These results revealed the magnitude of GR24 and TIS108 effects on hypocotyl elongation, showing that in Col-0 etiolated seedlings are less prone to GR24 compared to light-grown ones, while by contrast they were more responsive to TIS108 treatment. In addition, *max2-1* mutant was equally unresponsive to 3 μM GR24, but using 25 μM GR24 and 3 μM TIS108, etiolated seedlings exhibited a much stronger inhibitory effect.

4.2. Strigolactone effects on the organization of microtubules

It is well-known fact that the rearrangements of cytoskeleton, both microtubules and actin filaments, is the driving force of morphogenesis. Inducible growth alterations and exogenous hormonal treatments have been repeatedly shown to be preceded and supported by conditional rearrangements of cortical microtubules, which tend maintain their predominant orientation (e.g., Lindeboom et al., 2013; True and Shaw, 2020). Such conditions favoring the parallel arrangement of cortical microtubules can be documented by showing the patterns of their angular distribution and quantified by measuring the degree of anisotropy within the cortical array. In light/dark grown, mock-treated Col-0 seedlings carrying GFP-MBD microtubule marker, cortical microtubules exhibit a more or less random distribution (Figure 11A,E) with the tendency of more biased reorganization after treatment with 3 μM GR24 (Figure 11B,F), 25 μM GR24 (Figure 11C,G) and 3 μM TIS108 (Figure 11D,H).

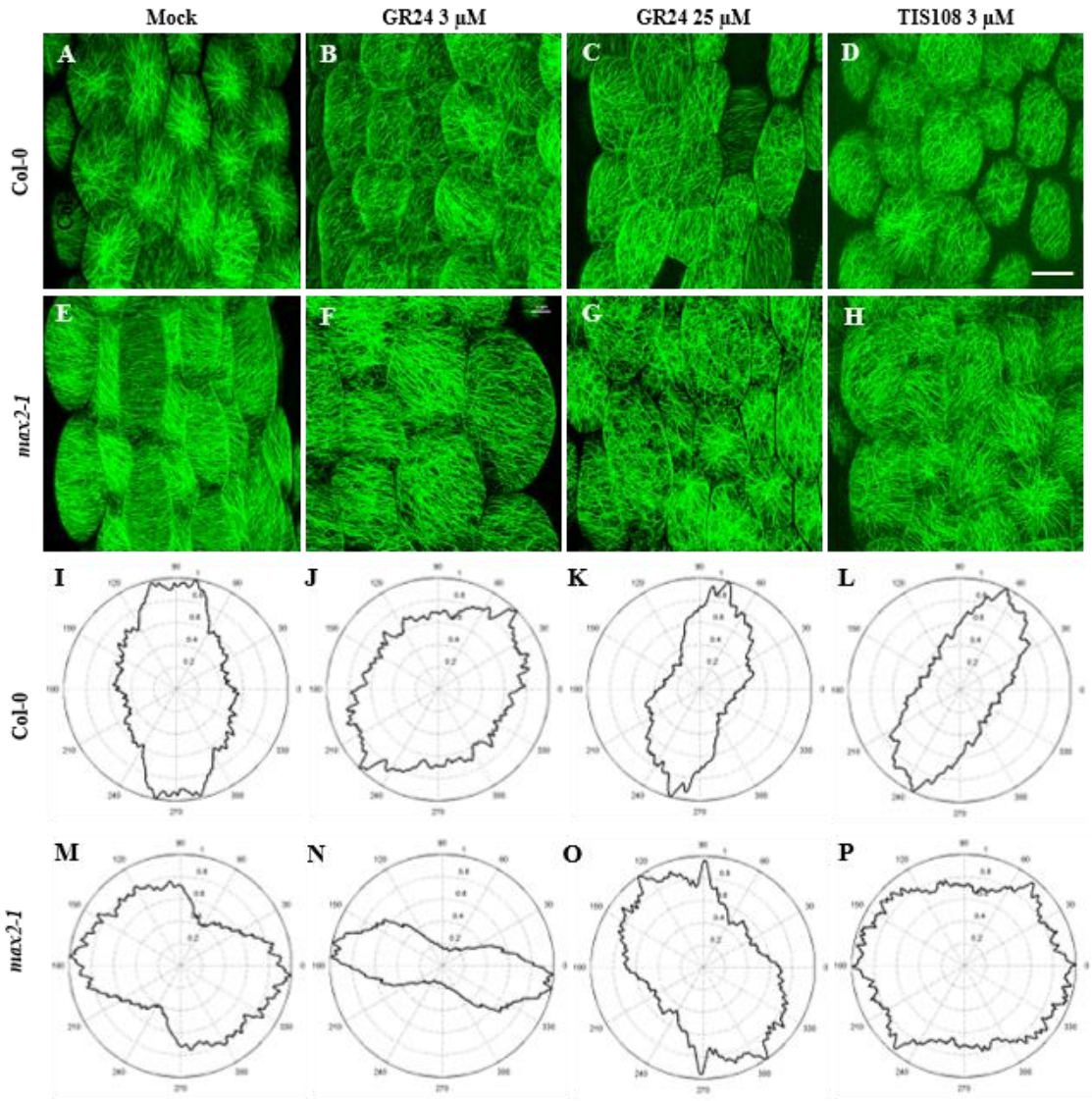

Figure 11. Cortical microtubule organization in hypocotyl epidermal cells of seedlings of *Arabidopsis thaliana* Col-0 or the *max2-1* mutant expressing the GFP-MBD microtubule marker and grown in standard light/dark regime without or with GR24 (3 and 25 µM) or 3 µM TIS108. (A-D) Epidermal hypocotyl cells of Col-0 seedlings treated with solvent alone (mock; A), 3 µM GR24 (B), 25 µM GR24 (C), and 3 µM TIS108 (D). (E-H) Hypocotyl epidermal cells of *max2-1* seedlings treated with solvent alone (mock; E), 3 µM GR24 (F), 25 µM GR24 (G), and 3 µM TIS108 (H). (I-L) Angular distribution analysis of cortical microtubules of Col-0 seedlings corresponding to (A) − (I); (B) − (J); (C) – (K) and (D) – (L), (H). (M-P) Angular distribution analysis of cortical microtubules of *max2-1* seedlings corresponding to (E) – (M), (F) – (N), (G) – (O), (H) – (P). Scale bars: 20 µm.

Max2-1 mutant expressing the GFP-MBD marker exhibited higher level of cortical microtubule organization by comparison to Col-0 either after mock (Figure 11I,M), 3 µM

GR24 (Figure 11J,N), 25 µM GR24 (Figure 11K,O) or 3 µM TIS108 (Figure 11L,P) treatments.

In etiolated seedlings of Col-0 bias of cortical microtubule organization was higher wehn compared to seedlings grown under a light/dark cycle. In controls (Figure 12A,E), the majority of cortical microtubules lied parallel to each other within the same cell, but at variable orientations compared to each other. However treatments with 3 µM GR24 (Figure 12B,F), 25 µM GR24 (Figure 12C,G) and 3 µM TIS108 (Figure 12D,H) did not appreciably change the propensity of highly ordered cortical microtubule arrangements.

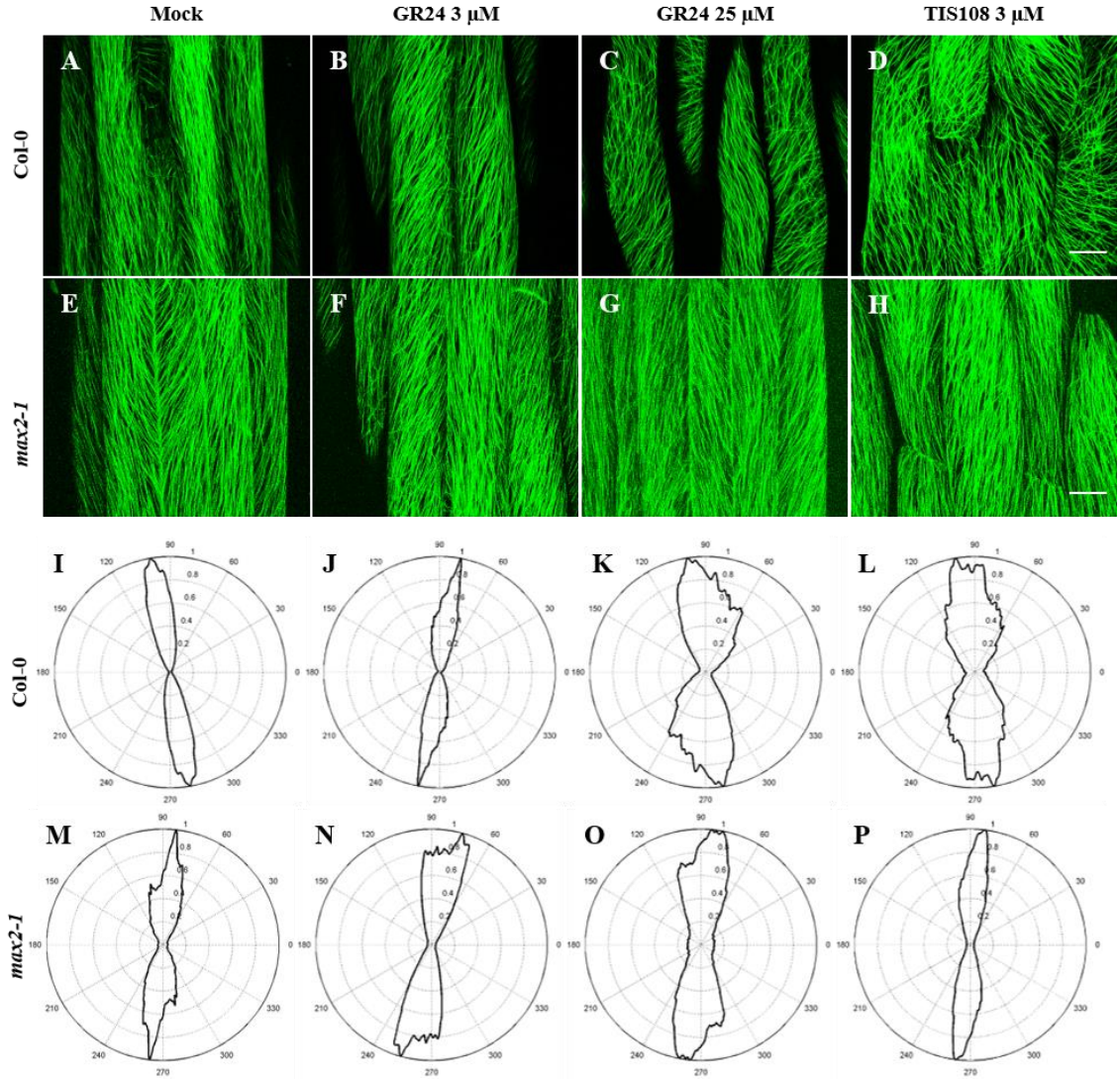

Figure 12. Assessment of microtubule organization in epidermal hypocotyl cells of etiolated seedlings of *Arabidopsis thaliana* (GFP-MBD) Col-0 or the *max2-1* mutant in the presence or absence of GR24 (3 and 25 µM) or TIS108 (3 µM). (A-D). Overview of hypocotyl of mock-treated Col-0 (A), or treated with 3 µM GR24 (B), 25 µM GR24 (C), and 3 µM TIS108 (D). Overview of hypocotyl of *max2-1* seedlings treated with solvent alone (mock; E), 3 µM GR24

(F), 25 μM GR24 (G), and 3 μM TIS108 (H). (I-L). Analysis of cortical microtubule angular distribution in Col-0 seedlings: (A) − (I); (B) − (J); (C) – (K) and (D) – (L), (M-P) Cortical microtubule angular distribution of *max2-1* seedlings corresponding to (E) – (M), (F) – (N), (G) – (O), (H) – (P). Scale bars: 20 μm.

Similarly to the wild type, the hypocotyl epidermal cells of etiolated max2-1 seedlings, exhibited highly organized systems of parallel microtubules, without noticeable changes to the degree of organization by comparison of control treatment (Figure 12 I,M) or treatments with 3 μM GR24 (Figure 12 J,N), 25 μM GR24 (Figure 12 K,O) and 3 μM TIS108 (Figure 12L,P). In both etiolated Col-0 and max2-1, the chemical interference with strigolactone synthesis or signaling does not seem to affect cortical microtubule organization.

4.3. Effects of strigolactones on actin organization

Cell growth control is also depending on the organization and dynamics of actin microfilaments. Exogenous GR24 application was shown to exert effects on actin organization and dynamics of root epidermal cells. Such effects were documented in TALIN or FABD2 reporter lines (Pandya-Kumar et al., 2014) both of which have been related to bundling of actin microfilaments (Ketelaar et al., 2004). Herein we rather followed actin organization in hypocotyls, after labeling with the Lifeact-GFP marker. The latter, is not expected to promote artificial actin organization in living cells (Riedl et al., 2008). WT Col-0 expressing Lifeact-GFP was used to document actin organization in hypocotyl cells of light/dark- or dark-grown seedlings after treatment with mock, or exogenous application of GR24 (3 μM and 25 μM) or TIS108 (3 μM).

To characterize actin organization, two measures were extrapolated: (a) skewness of fluorescence frequency distribution (accounting for actin bundling) and (b) occupancy of fluorescence per unit are (to deduce on the amount of polymeric actin). In light/dark grown mock-treated Col-0 seedlings actin microfilaments were evenly distributed in the cell cortex and seemingly the patterns of actin organization were very similar in hypocotyl cells treated with 3 μM GR24 (Figure 13B), 25 μM GR24 (Figure 13C) and 3 μM TIS108

(Figure 13D).

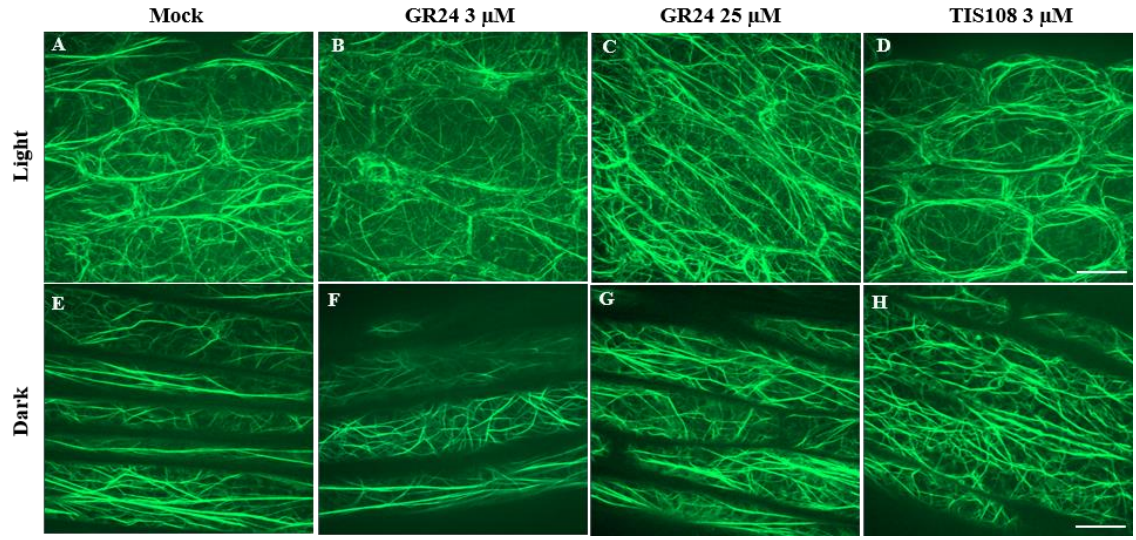

Figure 13. Organization of actin microfilaments in epidermal hypocotyl cells of light-grown seedlings of Col-0 expressing Lifeact-GFP before or after treatment with 3 µM and 25 µM GR24 or 3 µM TIS108. (A-D). Actin organization in light-grown, mock-treated Col-0 seedlings (A), or after treatment with 3 µM GR24 (B), 25 µM GR24 (C), and 3 µM TIS108 (D). (E-H) Actin organization in etiolated hypocotyl cells of Col-0 seedlings treated with solvent (E), 3 µM GR24 (F), 25 µM GR24 (G), and 3 µM TIS108 (H).

In etiolated hypocotyls, microfilaments are mostly organized in few robust longitudinal bundles. This actin organization trend does not change appreciably in mock-treated seedlings (Figure 13E), or following treatments with 3 µM GR24 (Figure 13F), 25 µM GR24 (Figure 13G) and 3 µM TIS108 (Figure 13H). Regardless the illumination mode, all treatments subtly affected occupancy (Table 1), when compared to controls.

Table 1. Quantification of actin occupancy and skewness in light and dark conditions in Col-0 hypocotyl epidermal cells.

	Light			
	mock	**GR24 3 µM**	**GR24 25 µM**	**TIS108 3 µM**
Occupancy (mean±SD)	3.67±2.07	3.44±1.70	2.96±1.57	4.713± 2.69
Skeweness (mean±SD)	2.45±0.51	2.497±0.54	2.158±0.38	2.38±0.58
	Dark			
	mock	**GR24 3 µM**	**GR24 25 µM**	**TIS108 3 µM**
Occupancy (mean±SD)	2.48±2.00	3.579±1.87	4.54±2.77	2.10±0.96
Skeweness (mean±SD)	3.60±0.99	3.71±0.71	2.86±0.52	3.12±0.67

On the other hand, fluorescence distribution skewness was more concretely stable under light/dark growth conditions, but was prone to changes in etiolated seedlings (Table 1). To summarize, occupancy is comparable between both groups at all experimental conditions (Figure 13M). On the other hand, actin filament bundling is higher after any treatment, compared to the light/dark grown ones (Table 1). Therefore, any difference in both terms of actin organization between light and dark-grown hypocotyls are not considerably affected by manipulation of strigolactone signaling.

4.3.1. Effects of strigolactones on actin dynamics and acquosomes formation

Actin dynamics were followed in Col-0 seedlings stably expressing a 35S::FABD-GFP construct in order to label actin microfilaments and actin bundles in the absence of artificial bundle formation caused by other markers such as fluorescent protein fusions of TALIN as was reported in previous studies (Ketelaar et al., 2004). In light-grown seedlings, visual comparison of provided time series of actin dynamics, showed that when compared to the mock treatment (Figure 14 A), the treatment with 3 μM GR24 (Figure 14,B), 25 μM GR24 (Figure 14 C) or 3 μM TIS108 (Figure 14 D) slowed down actin dynamicity (respective supplementary videos will be shown in the thesis presentation).

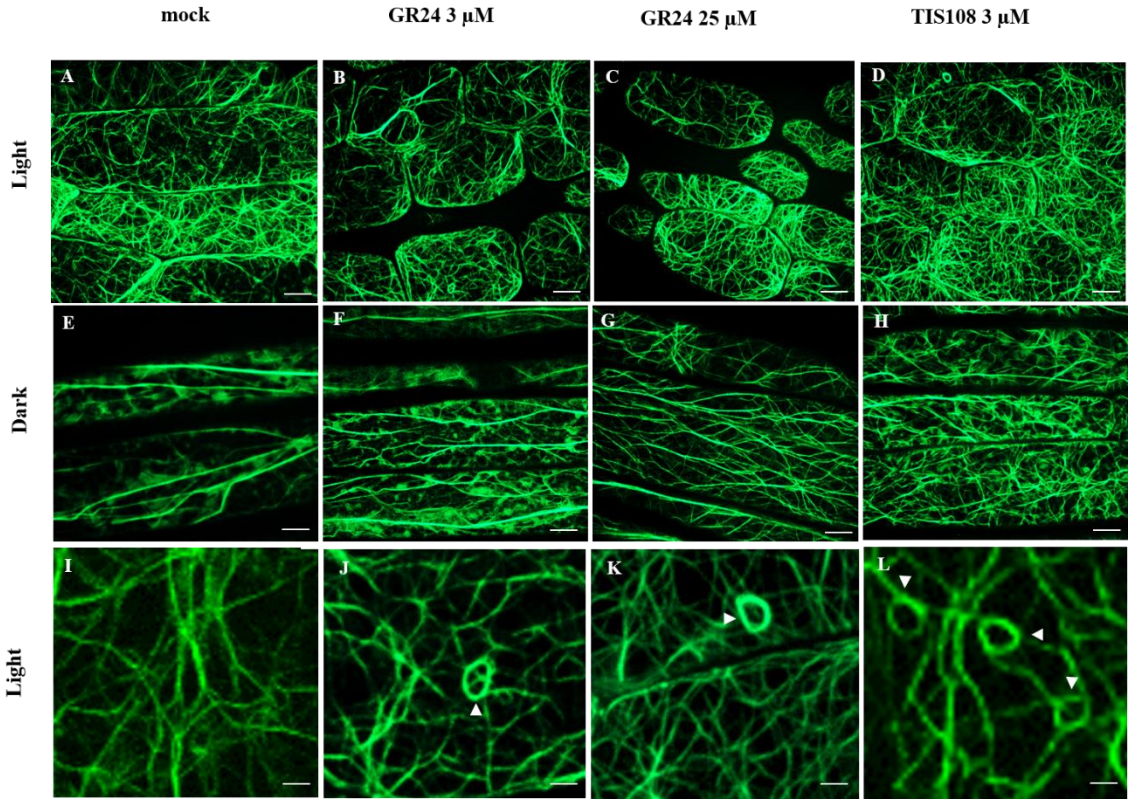

Figure 14. Assessment of actin filament organization in epidermal hypocotyl cells of light- (A-D) and dark- (E-H) grown seedlings of *Arabidopsis thaliana* Col-0 wild type expressing FABD2-GFP in the presence or absence of GR24 (3 μM and 25 μM) or TIS108 (3 μM). Formation of acquosomes (F-actin quoit-like structures) (arrowheads) in epidermal cells of hypocotyl cells of etiolated Col-0 seedlings in the presence of solvent alone (mock; I), 3 μM of GR24 (J), 25 μM of GR24 (K), and 3 μM of TIS108 (L). Scale bars: (A-H) 10 μm; (I-L) 5 μm.

By contrast, the highly vigorous actin dynamics of mock-treated dark-grown seedlings (Figure 14 E) stayed indifferent to either 3 μM GR24 (Figure 14 F), 25 μM GR24 (Figure 14 G), or μM of TIS108 (Figure 14 H). In turn, the number of acquosomes has been increasing with the increase of GR24 concentrations (Figure 14 J,K) and after TIS108 treatment as compared to mock-treated control (Figure 14 I), however, this observation has to be confirmed by the quantitative assessment.

5. DISCUSSION

Strigolactones are principally synthesized in roots (Ruyter-Spira et al., 2003). Thereon, they are transported to and regulate shoot (Gomez-Roldan et al., 2008; Umehara et al., 2008) and root (Ruyter-Spira et al., 2011; Hoffman et al., 2014). The transport of strigolactones from the root to the upper parts via the xylem, as proven in *Arabidopsis* and tomato gave clues regarding the regulation of strigolactone signaling by means of transport and organ-specific localization (Kohlen et al., 2011). Depending on the targeted organ, strigolactones may positively or negatively affect its size and number (rhizoid or caulonema; Hoffmann et al., 2014).

Herein, we examined implications of strigolactones in hypocotyl morphogenesis and growth by addressing their effects on actin and microtubule organization. Treatments with a synthetic strigolactone (GR24; Umehara et al., 2008) or chemical inhibition of strigolactone biosynthesis (TIS108; a potent triazole-containing inhibitor of cytochrome P450 monooxygenases; Ito et al., 2010, 2011, 2013), inhibited hypocotyl elongations in wild type Col-0 line and to a lesser extend in *max2-1*. This mutant exhibits reduced sensitivity to strigolactone signaling (Stirnberg et al., 2002; Wang et al., 2013, 2015). Conditional phenotypes of *max2* alleles include suppression of hypocotyl elongation inhibition, (Jia et al., 2014; Wang et al., 2020a), strigolactone-mediated shoot branching (Wang et al., 2013; Liu et al., 2014; Bennett et al., 2016; Li et al., 2016) and lateral root formation (Ruyter-Spira et al., 2013; Li et al., 2016). The function of MAX2 is rather

associated with light-perception processes rather than with strigolactone signaling per se (Lopez-Obando et al., 2018). As was shown before, GR24 representing an active synthetic strigolactone, inhibits the scotomorphogenic elongation of the hypocotyl and suppresses branch formation in both the shoot or the root. Finally, the effects of GR24 result to reduced tilling and compete auxin signaling against the formation of lateral roots (Ruyter- Spira et al., 2013; Jiang et al., 2016; Sun et al., 2019). In the present study, manipulation of strigolactone signaling was more pronounced in seedlings grown under light/dark conditions. Etiolated seedlings, were not indifferent to such treatments, but exhibited milder to negligible response to strigolactone manipulation. Hypocotyl elongation was previously shown to be impaired by exogenous strigolactone application in a dose-dependent manner, even at lower concentrations than those used herein (e.g., at 100 nM; Jia et al., 2014). In similar studies, *max2* mutant alleles exhibited negligible responses at low strigolactone doses and quantitative inhibition of hypocotyl elongation over 25 μM (Jia et al., 2014). In the present work, such results were confirmed, further delineating a correlation between strigolactone signaling modulation and seedling illumination (Brewer et al., 2013) possibly through phytochrome and cryptochrome light-dependent signaling (Jia et al., 2014).

Vegetative organ expansion largely relies on diffuse cell growth promoted by physical or hormonal signals. At the cellular level, growth directionality is associated with the positional control of cellulose microfibril deposition in the primary cell wall. Blueprinting of cellulose patterning is directly conducted by cortical microtubules and is fine tuned by actin microfilament organization. Cell, and eventually tissue and organ growth are related to environmental cues such as light (e.g., Sambade et al., 2012; Lindeboom et al., 2013; Ma et al., 2018) and mechanical stimulation (Louveaux et al., 2016; Takatani et al., 2020). Coordination of such physical stimuli and growth directionality along the whole plant body requires the effect of phytohormones including ethylene (Ma et al., 2018; Wang et al., 2020b), auxin (True and Shaw, 2020) and gibberellins (Vineyard et al., 2013; Locascio et al., 2013) on cytoskeletal organization and most importantly of cortical microtubules and actin (Zou et al., 2019; Arieti and Staiger, 2020).

Given the above information, we pursued the possibility that genetic and pharmacological interference with strigolactone signaling might be associated to conditional cytoskeletal reorganization. Thus, the organization of cortical microtubules were studied employing appropriate fluorescent markers and chemicals such as GR24 and TIS108 in both Col-0 and *max2-1* mutant. In terms of organization, exogenous

strigolactone application and inhibition of endogenous strigolactones biosynthesis under standard light/dark growth did not affect significantly cortical microtubule orientations in Col-0, but had a prominent effect in the *max2-1* mutant, promoting randomization in the cortical array.

Owing to the previous connection of strigolactones with phytochrome and cryptochrome light signaling pathways, the differential responses of cortical microtubules to strigolactone manipulation under light or dark growth conditions is expected. Earlier studies have already demonstrated the interdependence between phytochromes and light-induced microtubule reorientations (Fischer and Schopfer, 1997). More recently, the reorientation of cortical microtubules under blue light stimulation was attributed to the stimulation of KATANIN1-mediated microtubule severing by phototropins (Lindeboom et al., 2013). At present, the molecular components responsible for strigolactone-mediated suppression of microtubule dynamics remain unknown.

Surprisingly, actin organization both in light/dark- and dark-grown Col-0 seedlings proved to be more resistant to the application of GR24 and TIS108 as compared to microtubules. The only consistent and significant difference that was identified, was the higher degree of actin bundling in etiolated seedlings, which was again indifferent to exogenous manipulation of strigolactones.

On the other hand, actin dynamic rearrangements were strongly reduced by all treatments in light/dark-grown seedlings but remained virtually unaffected in etiolated ones. The only existing report on the effects of strigolactone signaling on actin organization and dynamics has addressed these aspects in the root (Pandya-Kumar et al., 2014), where by sharp contrast to the findings presented herein, GR24 application was found to loosen the actin microfilament systems and potentiate actin dynamicity. Interestingly, an actin mutant (*der1*) exhibited reduced sensitivity to GR24 (Pandya-Kumar et al., 2014). One possible explanation of the differences in the behavior of the actin cytoskeleton between the two studies may relate to the marker used to visualize the actin cytoskeleton. In the present work, actin microfilaments were tagged with a Lifeact-GFP-fusion, while the work of Pandya-Kumar and co-workers (2014) employed either a TALIN-GFP or a FABD2-GFP marker, both of which may promote artificial actin bundling (Ketelaar et al., 2004). Another plausible explanation may refer to the physiological differences between hypocotyls and roots, especially in relation to the interplay between strigolactone signaling and light perception. As mentioned previously, light-induced microtubule reorientations in aboveground tissues have been

shown to correlate with phytochrome (Zandomeni and Schopfer, 1993; Fischer and Schopfer, 1997) and phototropin (Lindeboom et al., 2013) signaling. The roots are also not indifferent to light, since dim light gradients may form at shallow depths of the soil and probably express specialized photoreceptors responsive to low light rates especially at the blue wavelength range (Galen et al., 2007 and references therein). Differences in photoreception between aboveground and soil-residing plant parts may explain differences in the cellular responses to strigolactones or strigolactone inhibitors and this is a matter that deserves to be followed up in future studies.

Although TIS108 is an inhibitor of P450 cytochrome monooxygenases and thus antagonist of strigolactone function, previous reports have confirmed its inhibitory effect on hypocotyl elongation (Kawada et al., 2019). Thus, the follow up effects of TIS108 on microtubule and actin organization and dynamics are in line with its observed effects on hypocotyl growth. Since the effects of TIS108 are also differentiated between light/dark-grown and etiolated seedlings, it is likely that the TIS108-induced cytoskeletal remodeling is also associated with imbalances in strigolactone signaling.

6. CONCLUSIONS

The main aim of this thesis was to characterize the effects of strigolactones as a novel class of phytohormones on the organization of cortical microtubules as well as the organization and dynamics of actin filaments. For this purpose, we exogenously applied GR24, a widely used synthetic strigolactone and TIS108, a potent triazole-containing inhibitor of cytochrome P450 monooxygenases involved in strigolactone biosynthesis on seedling hypocotyls of wild type *Arabidopsis thaliana* and strigolactone signaling mutant *max2-1*. To get an insight into the possible mechanisms of the cytoskeletal remodeling by strigolactones, we addressed organization of microtubules and actin filaments as well as actin filaments dynamics. In the search of cellular mechanisms underlying developmental functions of strigolactone signaling, the present study highlights the significance of cytoskeletal remodeling in the process of strigolactone-mediated growth inhibition of hypocotyl growth and reveals the differential regulation of microtubule and actin organization and dynamics by strigolactones at different illumination regimes. The following conclusions were drawn from the results of each experiment:

1) GR24 inhibited hypocotyl elongation of light-grown *Arabidopsis* Col-0 seedlings and induced mild radial swelling of epidermal cells as compared to mock-treated

seedlings, while *max2-1* hypocotyls were consistently longer as compared to similarly treated Col-0 ones.

2) SL biosynthesis inhibitor TIS108 caused evident hypocotyl growth inhibition of light-grown Col-0 and *max2-1* seedlings.
3) Hypocotyl width of light-grown Col-0 and *max2-1* seedlings was only mildly affected by any of the treatments used herein.
4) Generally, etiolated seedlings showed lower responsiveness to GR24, but higher responsiveness to TIS108 as compared to light-grown ones.
5) Cortical microtubules in cells of light-grown *Arabidopsis* (GFP-MBD) showed the tendency of more biased reorganization after GR24 and TIS108 treatments as compared to mock-treated Col-0 seedlings having a more or less random microtubules distribution. By contrast, light-grown *max2-1* mutant expressing the same microtubular marker appeared to have more organized cortical microtubules as compared to Col-0 either after mock, GR24 and TIS108 treatments.
6) In etiolated seedlings of Col-0 the degree of cortical microtubule organization was much more pronounced as compared to light-grown seedlings. Similarly, etiolated seedlings of the *max2-1* mutant exhibited highly organized systems of parallel microtubules at seemingly the same level of organization in any of the treatments used herein.
7) As compared to microtubules, actin organization both in light-grown and etiolated Col-0 seedlings proved to be more resistant to the application of GR24 and TIS108.
8) Light exposure strongly reduced actin bundling in all treatments, while in dark-grown seedlings these parameters remained predominantly unaffected.
9) The inhibitory effect of TIS108 on hypocotyl elongation and epidermal cell swelling are in line with the changes of microtubule and actin organization, possibly associated with fluctuations of strigolactones content.

After summarizing these results, we can conclude that strigolactones control cytoskeletal remodeling during the inhibition of hypocotyl elongation in a light-dependent manner.

7. REFERENCES

Aaziz, R., Dinant, S., and Epel, B. L. (2001): Plasmodesmata and plant cytoskeleton. *Trends in Plant Science* **6**, 326–330.

Abe, S., Sado, A., Tanaka, K., Kisugi, T., Asami, K., Ota, S., et al. (2014): Carlactone is converted to carlactonoic acid by MAX1 in *Arabidopsis* and its methyl ester can directly interact with AtD14 *in vitro*. PNAS **111**, 18084–18089.

Abeyaratne, R., Puntel, E., and Tomassetti, G. (2020): Treadmilling stability of a one-dimensional actin growth model. *International Journal of Solids and Structures* **198**, 87–98.

Agusti, J., Herold, S., Schwarz, M., Sanchez, P., Ljung, K., Dun, E. A., et al. (2011): Strigolactone signaling is required for auxin-dependent stimulation of secondary growth in plants. *PNAS* **108**, 20242–20247.

Akiyama, K., Matsuzaki, K., and Hayashi, H. (2005): Plant sesquiterpenes induce hyphal branching in arbuscular mycorrhizal fungi. *Nature* **435**, 824–827.

Akiyama, K., Ogasawara, S., Ito, S., and Hayashi, H. (2010): Structural requirements of strigolactones for hyphal branching in AM fungi. *Plant Cell Physiol* **51**, 1104–1117.

Al-Bassam, J., Kim, H., Brouhard, G., van Oijen, A., Harrison, S. C., and Chang, F. (2010): CLASP promotes microtubule rescue by recruiting tubulin dimers to the microtubule. *Dev Cell* **19**, 245–258.

Alushin, G. M., Lander, G. C., Kellogg, E. H., Zhang, R., Baker, D., and Nogales, E. (2014): High-resolution microtubule structures reveal the structural transitions in αβ-tubulin upon GTP hydrolysis. *Cell* **157**, 1117–1129.

Arieti, R. S., and Staiger, C. J. (2020): Auxin-induced actin cytoskeleton rearrangements require AUX1. *New Phytologist* **226**, 441–459.

Auldridge, M. E., Block, A., Vogel, J. T., Dabney-Smith, C., Mila, I., Bouzayen, M., et al. (2006): Characterization of three members of the *Arabidopsis* carotenoid cleavage dioxygenase family demonstrates the divergent roles of this multifunctional enzyme family. *The Plant Journal* **45**, 982–993.

Azimzadeh, J., Nacry, P., Christodoulidou, A., Drevensek, S., Camilleri, C., Amiour, N., et al. (2008): *Arabidopsis* TONNEAU1 proteins are essential for preprophase band formation and interact with centrin. *Plant Cell* **20**, 2146–2159.

Baluška, F., Barlow, P. W., and Volkmann, D. (1996): Complete disintegration of the microtubular cytoskeleton precedes its auxin-mediated reconstruction in postmitotic maize root cells. *Plant Cell Physiol* **37**, 1013–1021.

Baluška, F., Wojtaszek, P., Volkmann, D., and Barlow, P. (2003): The architecture of polarized cell growth: The unique status of elongating plant cells. *BioEssays* **25**, 569–576.

Bao, Y. Z., Yao, Z. Q., Cao, X. L., Peng, J. F., Xu, Y., Chen, M. X., et al. (2017): Transcriptome analysis of *Phelipanche aegyptiaca* seed germination mechanisms stimulated by fluridone, TIS108, and GR24. *PLOS ONE* 12.

Bennett, T., and Leyser, O. (2014): Strigolactone signalling: standing on the shoulders of DWARFs. *Current Opinion in Plant Biology* **22**, 7–13.

Bennett, T., Liang, Y., Seale, M., Ward, S., Müller, D., and Leyser, O. (2016a): Strigolactone regulates shoot development through a core signalling pathway. *Biology Open* **5**, 1806–1820.

Bennett, T., Liang, Y., Seale, M., Ward, S., Müller, D., and Leyser, O. (2016b): Strigolactone regulates shoot development through a core signalling pathway. *Biology Open* **5**, 1806–1820.

Berghöfer, T., Eing, C., Flickinger, B., Hohenberger, P., Wegner, L. H., Frey, W., et al. (2009): Nanosecond electric pulses trigger actin responses in plant cells. *Biochemical and Biophysical Research Communications* **387**, 590–595.

Blancaflor, E. B., and Hasenstein, K. H. (1995): Time course and auxin sensitivity of cortical microtubule reorientation in maize roots. *Protoplasma* **185**, 72–82.

Blanchoin, L., Boujemaa-Paterski, R., Henty, J. L., Khurana, P., and Staiger, C. J. (2010): Actin dynamics in plant cells: a team effort from multiple proteins orchestrates this very fast-paced game. *Current Opinion in Plant Biology* **13**, 714–723.

Blume, Y. B., Krasylenko, Y. A., Demchuk, O. M., and Yemets, A. I. (2013): Tubulin tyrosine nitration regulates microtubule organization in plant cells. *Front. Plant Sci.* **4**.

Blume, Y. B., Krasylenko, Y. A., and Yemets, A. I. (2017): "The role of the plant cytoskeleton in phytohormone signaling under abiotic and biotic stresses," in *Mechanism of plant hormone signaling under stress* (John Wiley & Sons, Ltd), 127–185.

Blume, Y. B., Lloyd, C. W., and Yemets, A. I. (2008): Plant tubulin phosphorylation and its role in cell cycle progression. in *The Plant Cytoskeleton: a Key Tool for Agro-Biotechnology* NATO Science for Peace and Security Series C: Environmental Security., eds. Y. B. Blume, W. V. Baird, A. I. Yemets, and D. Breviario (Dordrecht: Springer Netherlands), 145–159.

Blume, Y., Yemets, A., Sheremet, Y., Nyporko, A., Sulimenko, V., Sulimenko, T. (2010): Exposure of beta-tubulin regions defined by antibodies on an *Arabidopsis thaliana* microtubule protofilament model and in the cells. *BMC Plant Biol* **10**, 29.

Booker, J., Auldridge, M., Wills, S., McCarty, D., Klee, H., and Leyser, O. (2004): MAX3/CCD7 is a Carotenoid Cleavage Dioxygenase required for the synthesis of a novel plant signaling molecule. *Current Biology* **14**, 1232–1238.

Booker, J., Sieberer, T., Wright, W., Williamson, L., Willett, B., Stirnberg, P., et al. (2005): MAX1 encodes a Cytochrome P450 family member that acts downstream of MAX3/4 to produce a Carotenoid-Derived Branch-Inhibiting hormone. *Developmental Cell* **8**, 443–449.

Braun, M., Hauslage, J., Czogalla, A., and Limbach, C. (2004): Tip-localized actin polymerization and remodeling, reflected by the localization of ADF, profilin and villin, are fundamental for gravity-sensing and polar growth in characean rhizoids. *Planta* **219**, 379–388.

Brewer, P. B., Koltai, H., and Beveridge, C. A. (2013): Diverse roles of strigolactones in plant development. *Mol Plant* **6**, 18–28.

Brewer, P. B., Yoneyama, K., Filardo, F., Meyers, E., Scaffidi, A., Frickey, T., et al. (2016): LATERAL BRANCHING OXIDOREDUCTASE acts in the final stages of strigolactone biosynthesis in *Arabidopsis*. *PNAS* **113**, 6301–6306.

Brouhard, G. J., and Rice, L. M. (2018): Microtubule dynamics: an interplay of biochemistry and mechanics. *Nat Rev Mol Cell Biol* **19**, 451–463.

Boudaoud, A., Burian, A., Borowska-Wykręt, D., Uyttewaal, M., Wrzalik, R., Kwiatkowska, D., et al. (2014): FibrilTool, an ImageJ plug-in to quantify fibrillar structures in raw microscopy images. *Nature Protocols* **9**, 457–463.

Cai, G. (2010): Assembly and disassembly of plant microtubules: tubulin modifications and binding to MAPs. *J Exp Bot* **61**, 623–626.

Campellone, K. G., and Welch, M. D. (2010): A nucleator arms race: cellular control of actin assembly. *Nature Reviews Molecular Cell Biology* **11**, 237–251.

Chaaban, S., and Brouhard, G. J. (2017): A microtubule bestiary: structural diversity in tubulin polymers. *MBoC* **28**, 2924–2931.

Chen, F., Jiang, L., Zheng, J., Huang, R., Wang, H., Hong, Z., et al. (2014): Identification of differentially expressed proteins and phosphorylated proteins in rice seedlings in response to strigolactone treatment. *PLOS ONE* 9.

Cheng, X., Ruyter-Spira, C., and Bouwmeester, H. (2013): The interaction between strigolactones and other plant hormones in the regulation of plant development. *Front. Plant Sci.* **4**.

Chesarone, M. A., DuPage, A. G., and Goode, B. L. (2010): Unleashing formins to remodel the actin and microtubule cytoskeletons. *Nature Reviews Molecular Cell Biology* **11**, 62–74.

Chilley, P. M., Casson, S. A., Tarkowski, P., Hawkins, N., Wang, K. L.-C., Hussey, P. J., et al. (2006): The POLARIS peptide of *Arabidopsis* regulates auxin transport and root growth via effects on ethylene signaling. *The Plant Cell* **18**, 3058–3072.

Claassens, A. P., and Hills, P. N. (2018): "Effects of strigolactones on plant roots," in *Root Biology* Soil Biology., eds. B. Giri, R. Prasad, and A. Varma (Cham: Springer International Publishing), 43–63.

Cohen, M., Prandi, C., Occhiato, E. G., Tabasso, S., Wininger, S., Resnick, N., et al. (2013) Structure–function relations of strigolactone analogs: activity as plant hormones and plant interactions. *Molecular Plant* **6**, 141–152.

Conn, C. E., Bythell-Douglas, R., Neumann, D., Yoshida, S., Whittington, B., Westwood, J. H., et al. (2015). Convergent evolution of strigolactone perception enabled host detection in parasitic plants. *Science* **349**, 540–543.

Crawford, S., Shinohara, N., Sieberer, T., Williamson, L., George, G., Hepworth, J., et al. (2010): Strigolactones enhance competition between shoot branches by dampening auxin transport. *Development* **137**, 2905–2913.

de Saint Germain, A., Ligerot, Y., Dun, E. A., Pillot, J.-P., Ross, J. J., Beveridge, C. A., et al. (2013): Strigolactones stimulate internode elongation independently of gibberellins. *Plant Physiol.* **163**, 1012–1025.

Desai, A., and Mitchison, T. J. (1997): Microtubule polymerization dynamics. *Annual Review of Cell and Developmental Biology* **13**, 83–117.

Domagalska, M. A., and Leyser, O. (2011): Signal integration in the control of shoot branching. *Nature Reviews Molecular Cell Biology* **12**, 211–221.

Drøbak, B. K., Franklin-Tong, V. E., and Staiger, C. J. (2004): The role of the actin cytoskeleton in plant cell signaling. *New Phytologist* **163**, 13–30.

Duckett, C. M., and Lloyd, C. W. (1994): Gibberellic acid-induced microtubule reorientation in dwarf peas is accompanied by rapid modification of an α-tubulin isotype. *The Plant Journal* **5**, 363–372.

Elliott, A., and Shaw, S. L. (2018): Update: plant cortical microtubule arrays. *Plant Physiology* **176**, 94–105.

Eun, S.-O., Bae, S.-H., and Lee, Y. (2001): Cortical actin filaments in guard cells respond differently to abscisic acid in wild-type and abi1-1 mutant *Arabidopsis*. *Planta* **212**, 466–469.

Fischer, K., and Schopfer, P. (1997): Interaction of auxin, light, and mechanical stress in orienting microtubules in relation to tropic curvature in the epidermis of maize coleoptiles. *Protoplasma* **196**, 108–116.

Foo, E., Yoneyama, K., Hugill, C. J., Quittenden, L. J., and Reid, J. B. (2013): Strigolactones and the regulation of Pea symbioses in response to nitrate and phosphate deficiency. *Molecular Plant* **6**, 76–87.

Galjart, N. (2010): Plus-end-tracking proteins and their interactions at microtubule ends. *Current Biology* 20, R528–R537.

Gomez-Roldan, V., Fermas, S., Brewer, P. B., Puech-Pagès, V., Dun, E. A., Pillot, J.-P., et al. (2008a): Strigolactone inhibition of shoot branching. *Nature* **455**, 189–194.

Grabski, S., and Schindler, M. (1996): Auxins and cytokinins as antipodal modulators of elasticity within the actin network of plant cells. *Plant Physiology* **110**, 965–970.

Graumann, K., Vanrobays, E., Tutois, S., Probst, A. V., Evans, D. E., and Tatout, C. (2014): Characterization of two distinct subfamilies of SUN-domain proteins in *Arabidopsis* and their interactions with the novel KASH-domain protein AtTIK. *J Exp Bot* **65**, 6499–6512.

Grego, S., Cantillana, V., and Salmon, E. D. (2001): Microtubule treadmilling *in vitro* investigated by fluorescence speckle and confocal microscopy. *Biophysical Journal* **81**, 66–78.

Griffiths, J. S., Šola, K., Kushwaha, R., Lam, P., Tateno, M., Young, R., et al. (2015): Unidirectional movement of cellulose synthase complexes in *Arabidopsis* seed coat epidermal cells deposit cellulose involved in mucilage extrusion, adherence, and ray formation. *Plant Physiology* **168**, 502–520.

Ha, C. V., Leyva-González, M. A., Osakabe, Y., Tran, U. T., Nishiyama, R., Watanabe, Y., et al. (2014): Positive regulatory role of strigolactone in plant responses to drought and salt stress. *PNAS* **111**, 851–856.

Hamada, T. (2007): Microtubule-associated proteins in higher plants. *J Plant Res* 120, 79–98.

Hammond, J. W., Cai, D., and Verhey, K. J. (2008): Tubulin modifications and their cellular functions. *Current Opinion in Cell Biology* **20**, 71–76.

Hardham, A. R., Jones, D. A., and Takemoto, D. (2007): Cytoskeleton and cell wall function in penetration resistance. *Current Opinion in Plant Biology* **10**, 342–348.

Hardham, A. R., Takemoto, D., and White, R. G. (2008): Rapid and dynamic subcellular reorganization following mechanical stimulation of *Arabidopsis* epidermal cells mimics responses to fungal and oomycete attack. *BMC Plant Biology* **8**, 63.

Hauck, C., Müller, S., and Schildknecht, H. (1992): A Germination stimulant for parasitic flowering plants from *Sorghum bicolor*, a genuine host plant. *Journal of Plant Physiology* **139**, 474–478.

Higaki, T., Kutsuna, N., Sano, T., Kondo, N., and Hasezawa, S. (2010): Quantification and cluster analysis of actin cytoskeletal structures in plant cells: role of actin bundling in stomatal movement during diurnal cycles in *Arabidopsis* guard cells. *The Plant Journal* **61**, 156–165.

Hoffmann, B., Proust, H., Belcram, K., Labrune, C., Boyer, F.-D., Rameau, C., et al. (2014): Strigolactones inhibit caulonema elongation and cell division in the moss *Physcomitrella patens*. *PLOS ONE* 9.

Horio, T., and Murata, T. (2014): The role of dynamic instability in microtubule organization. *Front. Plant Sci.* 5.

Hu, Z., Yan, H., Yang, J., Yamaguchi, S., Maekawa, M., Takamure, I., et al. (2010): Strigolactones negatively regulate mesocotyl elongation in rice during germination and growth in darkness. *Plant Cell Physiol* **51**, 1136–1142.

Huang, S., Blanchoin, L., Kovar, D. R., and Staiger, C. J. (2003): *Arabidopsis* capping protein (AtCP) is a heterodimer that regulates assembly at the barbed ends of actin filaments. *J. Biol. Chem.* **278**, 44832–44842.

Hussey, P. J. (2009): *Annual Plant Reviews, The Plant Cytoskeleton in Cell Differentiation and Development*. John Wiley & Sons.

Hussey, P. J., Ketelaar, T., and Deeks, M. J. (2006): Control of the actin cytoskeleton in plant cell growth. *Annual Review of Plant Biology* **57**, 109–125.

Hwang, J. U., Suh, S., Yi, H., Kim, J., and Lee, Y. (1997): Actin filaments modulate both stomatal opening and inward K+-channel activities in guard cells of *Vicia faba* L. *Plant Physiology* **115**, 335–342.

Hwang, J.-U., and Lee, Y. (2001): Abscisic acid-induced actin reorganization in guard cells of dayflower is mediated by cytosolic calcium levels and by protein kinase and protein phosphatase activities. *Plant Physiology* **125**, 2120–2128.

Ito, S., Kitahata, N., Umehara, M., Hanada, A., Kato, A., Ueno, K., et al. (2010): A new lead chemical for strigolactone biosynthesis inhibitors. *Plant Cell Physiol* **51**, 1143–1150.

Ito, S., Umehara, M., Hanada, A., Kitahata, N., Hayase, H., Yamaguchi, S., et al. (2011): Effects of triazole derivatives on strigolactone levels and growth retardation in rice. *PLOS ONE* 6, e21723.

Ito, S., Umehara, M., Hanada, A., Yamaguchi, S., and Asami, T. (2013): Effects of strigolactone-biosynthesis inhibitor TIS108 on *Arabidopsis*. *Plant Signal Behav* 8.

Jamil, M., Kountche, B. A., Haider, I., Guo, X., Ntui, V. O., Jia, K.-P., et al. (2018): Methyl phenlactonoates are efficient strigolactone analogs with simple structure. *J Exp Bot* **69**, 2319–2331.

Jamil, M., Kountche, B. A., Wang, J. Y., Haider, I., Jia, K.-P., Takahashi, I., et al. (2020): a new series of carlactonoic acid based strigolactone analogs for fundamental and applied research. *Front. Plant Sci.* 11.

Janda, M., Matoušková, J., Burketová, L., and Valentová, O. (2014): Interconnection between actin cytoskeleton and plant defense signaling. *Plant Signal Behav* 9.

Janke, C., and Magiera, M. M. (2020): The tubulin code and its role in controlling microtubule properties and functions. *Nature Reviews Molecular Cell Biology*, 1–20.

Jia, K.-P., Kountche, B. A., Jamil, M., Guo, X., Ntui, V. O., Rüfenacht, A., et al. (2016). Nitro-phenlactone, a carlactone analog with pleiotropic strigolactone activities. *Mol Plant* **9**, 1341–1344.

Jia, K.-P., Luo, Q., He, S.-B., Lu, X.-D., and Yang, H.-Q. (2014): Strigolactone-regulated hypocotyl elongation is dependent on cryptochrome and phytochrome signaling pathways in *Arabidopsis*. *Molecular Plant* **7**, 528–540.

Job, D., Valiron, O., and Oakley, B. (2003): Microtubule nucleation. *Current Opinion in Cell Biology* **15**, 111–117.

Johnson, A. W., Gowada, G., Hassanali, A., Knox, J., Monaco, S., Razavi, Z., et al. (1981): The preparation of synthetic analogues of strigol. *J. Chem. Soc., Perkin Trans. **1***, 1734–1743.

Kapulnik, Y., Delaux, P.-M., Resnick, N., Mayzlish-Gati, E., Wininger, S., Bhattacharya, C., et al. (2011): Strigolactones affect lateral root formation and root-hair elongation in *Arabidopsis*. *Planta* **233**, 209–216.

Kartasalo, K., Pölönen, R.-P., Ojala, M., Rasku, J., Lekkala, J., Aalto-Setälä, K., et al. (2015): CytoSpectre: a tool for spectral analysis of oriented structures on cellular and subcellular levels. BMC Bioinformatics **16**, 344.

Ketelaar, T., Anthony, R. G., and Hussey, P. J. (2004): Green fluorescent protein-mTalin causes defects in actin organization and cell expansion in *Arabidopsis* and inhibits actin depolymerizing factor's actin depolymerizing activity in vitro. *Plant Physiol.* **136**, 3990–3998.

Kobayashi, Y., and Kobayashi, I. (2007): Depolymerization of the actin cytoskeleton induces defense responses in tobacco plants. *J Gen Plant Pathol* **73**, 360–364.

Beguerie, S., et al. (2011): Strigolactones are transported through the xylem and play a key role in shoot architectural response to phosphate deficiency in nonarbuscular mycorrhizal host *Arabidopsis*. *Plant Physiol.* **155**, 974–987.

Koltai, H. (2011): Strigolactones are regulators of root development. *New Phytologist* **190**, 545–549.

Koltai, H. (2014): Receptors, repressors, PINs: a playground for strigolactone signaling. *Trends in Plant Science* **19**, 727–733.

Komis, G., Apostolakos, P., and Galatis, B. (2002): Hyperosmotic stress-induced actin filament reorganization in leaf cells of *Chlorophyton comosum*. *J Exp Bot* **53**, 1699–1710.

Komis, G., Mistrik, M., Šamajová, O., Doskočilová, A., Ovečka, M., Illés, P., et al. (2014): Dynamics and organization of cortical microtubules as revealed by superresolution structured illumination microscopy. *Plant Physiology* **165**, 129–148.

Komis, G., Mistrik, M., Šamajová, O., Ovečka, M., Bartek, J., and Šamaj, J. (2015a): Superresolution live imaging of plant cells using structured illumination microscopy. *Nature Protocols* **10**, 1248–1263.

Komis, G., Šamajová, O., Ovečka, M., and Šamaj, J. (2015b): Super-resolution microscopy in plant cell imaging. *Trends in Plant Science* **20**, 834–843.

Kopczak, S. D., Haas, N. A., Hussey, P. J., Silflow, C. D., and Snustad, D. P. (1992): The small genome of *Arabidopsis* contains at least six expressed alpha-tubulin genes. *The Plant Cell* **4**, 539–547.

Koren, D., Resnick, N., Gati, E. M., Belausov, E., Weininger, S., Kapulnik, Y., et al. (2013): Strigolactone signaling in the endodermis is sufficient to restore root responses and involves SHORT HYPOCOTYL 2 (SHY2) activity. *New Phytologist* **198**, 866–874.

Krtková, J., Benáková, M., and Schwarzerová, K. (2016): Multifunctional microtubule-associated proteins in plants. *Front. Plant Sci.* 7.

Kumar, M., Pandya-Kumar, N., Dam, A., Haor, H., Mayzlish-Gati, E., Belausov, E., et al. (2015): *Arabidopsis* response to low-phosphate conditions includes active changes in actin filaments and PIN2 polarization and is dependent on strigolactone signalling. *J Exp Bot* **66**, 1499–1510.

Lachia, M., Wolf, H. C., Jung, P. J. M., Screpanti, C., and De Mesmaeker, A. (2015): Strigolactam: New potent strigolactone analogues for the germination of *Orobanche cumana*. *Bioorganic & Medicinal Chemistry Letters* **25**, 2184–2188.

Lee, Y.-R. J., and Liu, B. (2019): Microtubule nucleation for the assembly of acentrosomal microtubule arrays in plant cells. *New Phytologist* **222**, 1705–1718.

Li, H., Sun, B., Sasabe, M., Deng, X., Machida, Y., Lin, H., et al. (2017): *Arabidopsis* MAP65-4 plays a role in phragmoplast microtubule organization and marks the cortical cell division site. *New Phytol.* **215**, 187–201.

Li, J., Blanchoin, L., and Staiger, C. J. (2015): Signaling to actin stochastic dynamics. *Annual Review of Plant Biology* **66**, 415–440.

Li, W., Nguyen, K. H., Watanabe, Y., Yamaguchi, S., and Tran, L.-S. P. (2016): OaMAX2 of *Orobanche aegyptiaca* and *Arabidopsis* AtMAX2 share conserved functions in both development and drought responses. *Biochem. Biophys. Res. Commun.* **478**, 521–526.

Li, X., Sun, S., Li, C., Qiao, S., Wang, T., Leng, L., et al. (2014): The Strigolactone-related mutants have enhanced lamina joint inclination phenotype at the seedling stage. *Journal of Genetics and Genomics* **41**, 605–608.

Lindeboom, J. J., Nakamura, M., Hibbel, A., Shundyak, K., Gutierrez, R., Ketelaar, T., et al. (2013): A mechanism for reorientation of cortical microtubule arrays driven by microtubule severing. *Science* **342**, 1245533.

Locascio, A., Blázquez, M. A., and Alabadí, D. (2013): Dynamic regulation of cortical microtubule organization through prefoldin-DELLA interaction. *Curr. Biol.* **23**, 804–809.

Lopez-Obando, M., de Villiers, R., Hoffmann, B., Ma, L., de Saint Germain, A., Kossmann, J., et al. (2018): *Physcomitrella patens* MAX2 characterization suggests an

ancient role for this F-box protein in photomorphogenesis rather than strigolactone signalling. *New Phytol.* **219**, 743–756.

López-Ráez, J. A., Shirasu, K., and Foo, E. (2017): Strigolactones in plant interactions with beneficial and detrimental organisms: The Yin and Yang. *Trends in Plant Science* **22**, 527–537.

Louveaux, M., Rochette, S., Beauzamy, L., Boudaoud, A., and Hamant, O. (2016): The impact of mechanical compression on cortical microtubules in *Arabidopsis*: a quantitative pipeline. *Plant J.* **88**, 328–342.

Lu, Y.-J., and Day, B. (2017): "Quantitative evaluation of plant actin cytoskeletal organization during immune signaling," in *Plant Pattern Recognition Receptors* Methods in Molecular Biology., eds. L. Shan and P. He (New York, NY: Springer New York), 207–221.

Lucas, J., and Shaw, S. L. (2008): Cortical microtubule arrays in the Arabidopsis seedling. *Curr. Opin. Plant Biol.* **11**, 94–98.

Lumba, S., Bunsick, M., and McCourt, P. (2017): Chemical genetics and strigolactone perception. *F1000Res* 6.

Ma, H. (2005): Molecular genetic analyses of microsporogenesis and microgametogenesis in flowering plants. Annual Review of Plant Biology **56**, 393–434

Madmon, O., Mazuz, M., Kumari, P., Dam, A., Ion, A., Mayzlish-Gati, E., et al. (2016): Expression of MAX2 under SCARECROW promoter enhances the strigolactone/MAX2 dependent response of *Arabidopsis* roots to low-phosphate conditions. *Planta* **243**, 1419–1427.

Mandelkow, E. M., Mandelkow, E., and Milligan, R. A. (1991): Microtubule dynamics and microtubule caps: a time-resolved cryo-electron microscopy study. *J Cell Biol* **114**, 977–991.

Marc, J., Granger, C., Brincat, J., Fisher, D., Kao, T., McCubbin, A., et al. (1998): A GFP-MAP4 reporter gene for visualizing cortical microtubule rearrangements in living epidermal cells. *Plant Cell* 10**,** 1927–1940.

Martinez, P., Luo, A., Sylvester, A., and Rasmussen, C. G. (2017): Proper division plane orientation and mitotic progression together allow normal growth of maize. *PNAS* **114**, 2759–2764.

Masoud, K., Herzog, E., Chabouté, M.-E., and Schmit, A.-C. (2013): Microtubule nucleation and establishment of the mitotic spindle in vascular plant cells. *The Plant Journal* **75**, 245–257.

Matoušková, J., Janda, M., Fišer, R., Šašek, V., Kocourková, D., Burketová, L., et al. (2014): Changes in actin dynamics are involved in salicylic acid signaling pathway. *Plant Science* **223**, 36–44.

Mayzlish-Gati, E., Laufer, D., Grivas, C. F., Shaknof, J., Sananes, A., Bier, A., et al. (2015): Strigolactone analogs act as new anti-cancer agents in inhibition of breast cancer in xenograft model. *Cancer Biology & Therapy* **16**, 1682–1688.

Mitchison, T., and Kirschner, M. (1984): Dynamic instability of microtubule growth. *Nature* **312**, 237–242.

Molines, A. T., Marion, J., Chabout, S., Besse, L., Dompierre, J. P., Mouille, G., et al. (2018): EB1 contributes to microtubule bundling and organization, along with root growth, in *Arabidopsis thaliana*. *Biology Open* 7.

Murray, J. D. (2011): Invasion by Invitation: Rhizobial Infection in Legumes. *MPMI* **24**, 631–639.

Najafpour, M. (2012): *Advances in Photosynthesis: Fundamental Aspects*. BoD – Books on Demand.

Nakajima, K., Kawamura, T., and Hashimoto, T. (2006): Role of the SPIRAL1 Gene family in anisotropic growth of *Arabidopsis thaliana*. *Plant Cell Physiol* **47**, 513–522.

Nick, P. (2008): "Microtubules as sensors for abiotic stimuli," in *Plant Microtubules: Development and Flexibility* Plant Cell Monographs., ed. P. Nick (Berlin, Heidelberg: Springer), 175–203.

Nick, P. (2013): Microtubules, signalling and abiotic stress. *The Plant Journal* **75**, 309–323.

Nogales, E. (2015). An electron microscopy journey in the study of microtubule structure and dynamics. *Protein Science* **24**, 1912–1919.

Palmieri, M., and Kiss, J. Z. (2005): Disruption of the F-actin cytoskeleton limits statolith movement in Arabidopsis hypocotyls. *J Exp Bot* **56**, 2539–2550.

Pandya-Kumar, N., Shema, R., Kumar, M., Mayzlish-Gati, E., Levy, D., Zemach, H., et al. (2014): Strigolactone analog GR24 triggers changes in PIN2 polarity, vesicle trafficking and actin filament architecture. *New Phytologist* **202**, 1184–1196.

Paradez, A., Wright, A., and Ehrhardt, D. W. (2006): Microtubule cortical array organization and plant cell morphogenesis. *Current Opinion in Plant Biology* **9**, 571–578.

Plohovska, S. G., Yemets, A. I., and Blume, Ya. B. (2016): Influence of cold on organization of actin filaments of different types of root cells in *Arabidopsis thaliana*. *Cytol. Genet.* **50**, 318–323.

Pollock, C. B., McDonough, S., Wang, V. S., Lee, H., Ringer, L., Li, X., et al. (2014): Strigolactone analogues induce apoptosis through activation of p38 and the stress response pathway in cancer cell lines and in conditionally reprogramed primary prostate cancer cells. *Oncotarget* **5**, 1683–1698.

Porter, K., and Day, B. (2016): From filaments to function: The role of the plant actin cytoskeleton in pathogen perception, signaling and immunity. *J Integr Plant Biol* **58**, 299–311.

Rahman, A., Bannigan, A., Sulaman, W., Pechter, P., Blancaflor, E. B., and Baskin, T. I. (2007): Auxin, actin and growth of the *Arabidopsis thaliana* primary root. *The Plant Journal* **50**, 514–528.

Rasmussen, A., Heugebaert, T., Matthys, C., Van Deun, R., Boyer, F.-D., Goormachtig, S., et al. (2013): A Fluorescent alternative to the synthetic strigolactone GR24. *Molecular Plant* **6**, 100–112.

Riedl, J., Crevenna, A. H., Kessenbrock, K., Yu, J. H., Neukirchen, D., Bista, M., et al. (2008a): Lifeact: a versatile marker to visualize F-actin. *Nat. Methods* **5**, 605–607.

Riedl, J., Crevenna, A. H., Kessenbrock, K., Yu, J. H., Neukirchen, D., Bista, M., et al. (2008b): Lifeact: a versatile marker to visualize F-actin. *Nature Methods* **5**, 605–607.

Roberts, I. N., Lloyd, C. W., and Roberts, K. (1985): Ethylene-induced microtubule reorientations: mediation by helical arrays. *Planta* **164**, 439–447.

Roumeliotis, E., Kloosterman, B., Oortwijn, M., Kohlen, W., Bouwmeester, H. J., Visser, R. G. F., et al. (2012): The effects of auxin and strigolactones on tuber initiation and stolon architecture in potato. J Exp Bot **63**, 4539–4547.

Ruggenthaler, P., Fichtenbauer, D., Krasensky, J., Jonak, C., and Waigmann, E. (2009): microtubule-associated protein AtMPB2C plays a role in organization of cortical microtubules, stomata patterning, and tobamovirus infectivity. *Plant Physiol* **149**, 1354–1365.

Ruyter-Spira, C., Al-Babili, S., van der Krol, S., and Bouwmeester, H. (2013): The biology of strigolactones. *Trends Plant Sci*. **18**, 72–83.

Ruyter-Spira, C., Kohlen, W., Charnikhova, T., Zeijl, A. van, Bezouwen, L. van, Ruijter, N. de, et al. (2011): Physiological effects of the synthetic strigolactone analog GR24 on root system architecture in *Arabidopsis*: another belowground role for strigolactones? *Plant Physiology* **155**, 721–734.

Saeed, W., Naseem, S., and Ali, Z. (2017): Strigolactones biosynthesis and their role in abiotic stress resilience in plants: A Critical Review. *Front. Plant Sci.* 8.

Sambade, A., Pratap, A., Buschmann, H., Morris, R. J., and Lloyd, C. (2012). The influence of light on microtubule dynamics and alignment in the *Arabidopsis* hypocotyl. *Plant Cell* **24**, 192–201.

Sampathkumar, A., Gutierrez, R., McFarlane, H. E., Bringmann, M., Lindeboom, J., Emons, A.-M., et al. (2013). Patterning and lifetime of plasma membrane-localized cellulose synthase is dependent on actin organization in *Arabidopsis* interphase cells. *Plant Physiology* **162**, 675–688.

Scaffidi, A., Waters, M. T., Sun, Y. K., Skelton, B. W., Dixon, K. W., Ghisalberti, E. L., et al. (2014): Strigolactone hormones and their stereoisomers signal through two related receptor proteins to induce different physiological responses in *Arabidopsis*. *Plant Physiology* **165**, 1221–1232.

Schmelzer, E. (2002): Cell polarization, a crucial process in fungal defense. *Trends in Plant Science* **7**, 411–415.

Schmidt, S. M., and Panstruga, R. (2007): Cytoskeleton functions in plant–microbe interactions. *Physiological and Molecular Plant Pathology* 71, 135–148.

Schoenaers, S., Balcerowicz, D., and Vissenberg, K. (2017): "Molecular mechanisms regulating root hair tip growth: a comparison with pollen tubes," in *Pollen Tip Growth: From Biophysical Aspects to Systems Biology*.

Seto, Y., and Yamaguchi, S. (2014): Strigolactone biosynthesis and perception. *Current Opinion in Plant Biology* **21**, 1–6.

Shaw, S. L., Kamyar, R., and Ehrhardt, D. W. (2003): Sustained microtubule treadmilling in *Arabidopsis* cortical arrays. *Science* 300, 1715–1718.

Shinohara, N., Taylor, C., and Leyser, O. (2013): Strigolactone can promote or inhibit shoot branching by triggering rapid depletion of the auxin efflux protein PIN1 from the plasma membrane. *PLOS BIOL*. 11, e1001474.

Siame, B. A., Weerasuriya, Yohan., Wood, Karl., Ejeta, Gebisa., and Butler, L. G. (1993): Isolation of strigol, a germination stimulant for *Striga asiatica*, from host plants. *J. Agric. Food Chem.* **41**, 1486–1491.

Silacci, P., Mazzolai, L., Gauci, C., Stergiopulos, N., Yin, H. L., and Hayoz, D. (2004): Gelsolin superfamily proteins: key regulators of cellular functions. *CMLS, Cell. Mol. Life Sci.* **61**, 2614–2623.

Smertenko, A., Blume, Y., Viklický, V., Opatrný, Z., and Dráber, P. (1997a): Post-translational modifications and multiple tubulin isoforms in *Nicotiana tabacum* L. cells. *Planta* **201**, 349–358.

Smertenko, A., Dráber, P., Viklický, V., and Opatrný, Z. (1997b): Heat stress affects the organization of microtubules and cell division in *Nicotiana tabacum* cells. *Plant, Cell & Environment* **20**, 1534–1542.

Smertenko, A., Hewitt, S. L., Jacques, C. N., Kacprzyk, R., Liu, Y., Marcec, M. J., et al. (2018): Phragmoplast microtubule dynamics - a game of zones. *J. Cell. Sci.* 131.

Smertenko, A. P., Deeks, M. J., and Hussey, P. J. (2010): Strategies of actin reorganisation in plant cells. *J Cell Sci* **123**, 3019–3028.

Smith, S. M., and Li, J. (2014): Signalling and responses to strigolactones and karrikins. *Current Opinion in Plant Biology* **21**, 23–29.

Soto, M. J., Fernández-Aparicio, M., Castellanos-Morales, V., García-Garrido, J. M., Ocampo, J. A., Delgado, M. J., et al. (2010): First indications for the involvement of strigolactones on nodule formation in alfalfa (*Medicago sativa*). *Soil Biology and Biochemistry* **42**, 383–385.

Soundappan, I., Bennett, T., Morffy, N., Liang, Y., Stanga, J. P., Abbas, A., et al. (2015): SMAX1-LIKE/D53 family members enable distinct MAX2-dependent responses to strigolactones and karrikins in *Arabidopsis*. The Plant Cell **27**, 3143–3159.

Sparkes, I. A., Ketelaar, T., Ruijter, N. C. A. D., and Hawes, C. (2009): Grab a Golgi: Laser trapping of golgi bodies reveals *in vivo* interactions with the endoplasmic reticulum. *Traffic* **10**, 567–57.

Sparkes, I., Hawes, C., and Frigerio, L. (2011): FrontiERs: movers and shapers of the higher plant cortical endoplasmic reticulum. *Current Opinion in Plant Biology* **14**, 658–665.

Stanga, J. P., Smith, S. M., Briggs, W. R., and Nelson, D. C. (2013): SUPPRESSOR OF MORE AXILLARY GROWTH2 1 controls seed germination and seedling development in *Arabidopsis*. *Plant Physiology* **163**, 318–330.

Steinkellner, S., Lendzemo, V., Langer, I., Schweiger, P., Khaosaad, T., Toussaint, J.-P., et al. (2007): Flavonoids and strigolactones in root exudates as signals in symbiotic and pathogenic plant-fungus interactions. *Molecules* **12**, 1290–1306.

Stirnberg, P., Sande, K. van de, and Leyser, H. M. O. (2002a): MAX1 and MAX2 control shoot lateral branching in *Arabidopsis*. *Development* **129**, 1131–1141.

Suetsugu, N., and Wada, M. (2012): Chloroplast photorelocation movement: A sophisticated strategy for chloroplasts to perform efficient photosynthesis. advances in photosynthesis - fundamental aspects.

Sun, H., Tao, J., Hou, M., Huang, S., Chen, S., Liang, Z., et al. (2015): A strigolactone signal is required for adventitious root formation in rice. *Ann Bot* **115**, 1155–1162.

Szymanski, D. (2002): Tubulin folding cofactors: half a dozen for a dimer. *Current Biology* **12**, 767–769.

Takatani, S., Verger, S., Okamoto, T., Takahashi, T., Hamant, O., and Motose, H. (2020): microtubule response to tensile stress is curbed by NEK6 to buffer growth variation in the *Arabidopsis* hypocotyl. *Curr. Biol.* **30**, 1491-1503.e2.

Takemoto, D., and Hardham, A. R. (2004): The Cytoskeleton as a regulator and target of biotic interactions in plants. *Plant Physiology* **136**, 3864–3876.

Takesue, K., and Shibaoka, H. (1999): Auxin-induced longitudinal-to-transverse reorientation of cortical microtubules in non-elongating epidermal cells of azuki bean epicotyls. *Protoplasma* **206**, 27–30.

Thomas, S. G., Huang, S., Li, S., Staiger, C. J., and Franklin-Tong, V. E. (2006): Actin depolymerization is sufficient to induce programmed cell death in self-incompatible pollen. *J Cell Biol* **174**, 221–229.

Timofeeva, O., Khokhlova, L., Belyaeva, N., Chulkova, Y., and Garaeva, L. (2000): Cytoskeleton-induced alterations of the lectin activity in winter wheat under cold hardening and abscisic acid (aba). *Cell Biology International* **24**, 375–381.

True, J. H., and Shaw, S. L. (2020): Exogenous auxin induces transverse microtubule arrays through TRANSPORT INHIBITOR RESPONSE1/AUXIN SIGNALING F-BOX receptors. *Plant Physiology* **182**, 892–907.

Tsuchiya, Y., Vidaurre, D., Toh, S., Hanada, A., Nambara, E., Kamiya, Y., et al. (2010): A small-molecule screen identifies new functions for the plant hormone strigolactone. *Nature Chemical Biology* **6**, 741–749.

Turnbull, C. G. N., Booker, J. P., and Leyser, H. M. O. (2002): Micrografting techniques for testing long-distance signalling in *Arabidopsis*. *The Plant Journal* **32**, 255–262.

Umehara, M., Hanada, A., Yoshida, S., Akiyama, K., Arite, T., Takeda-Kamiya, N., et al. (2008): Inhibition of shoot branching by new terpenoid plant hormones. *Nature* **455**, 195–200.

Valster, A. H., Pierson, E. S., Valenta, R., Hepler, P. K., and Emons, A. (1997): Probing the plant actin cytoskeleton during cytokinesis and interphase by profilin microinjection. *The Plant Cell* **9**, 1815–1824.

Verde, F., Dogterom, M., Stelzer, E., Karsenti, E., and Leibler, S. (1992): Control of microtubule dynamics and length by cyclin A- and cyclin B-dependent kinases in Xenopus egg extracts. *J Cell Biol* **118**, 1097–1108.

Vineyard, L., Elliott, A., Dhingra, S., Lucas, J. R., and Shaw, S. L. (2013): Progressive transverse microtubule array organization in hormone-induced *Arabidopsis* hypocotyl cells. *Plant Cell* **25**, 662–676.

Voigt, B., Timmers, A. C. J., Šamaj, J., Müller, J., Baluška, F., and Menzel, D. (2005): GFP-FABD2 fusion construct allows *in vivo* visualization of the dynamic actin cytoskeleton in all cells of *Arabidopsis* seedlings. European Journal of Cell Biology **84**, 595–608.

Wakefield, J. G., Moores, C. A., Zwetsloot, A. J., Tut, G., and Straube, A. (2018): Measuring microtubule dynamics. *Essays Biochem* **62**, 725–735.

Wang, L., Wang, B., Jiang, L., Liu, X., Li, X., Lu, Z., et al. (2015): Strigolactone signaling in *Arabidopsis* regulates shoot development by targeting D53-Like SMXL repressor proteins for ubiquitination and degradation. *Plant Cell* **27**, 3128–3142.

Wang, L., Xu, Q., Yu, H., Ma, H., Li, X., Yang, J., et al. (2020): Strigolactone and karrikin signaling pathways elicit ubiquitination and proteolysis of SMXL2 to regulate hypocotyl elongation in *Arabidopsis thaliana*. *Plant Cell*.

Wang, Q.-Y., and Nick, P. (1998): The auxin response of actin is altered in the rice mutant Yin-Yang. *Protoplasma* **204**, 22–33.

Wang, Y., Sun, S., Zhu, W., Jia, K., Yang, H., and Wang, X. (2013): Strigolactone/MAX2-induced degradation of brassinosteroid transcriptional effector BES1 regulates shoot branching. *Dev. Cell* **27**, 681–688.

Wasteneys, G. O. (2002): Microtubule organization in the green kingdom: chaos or self-order? *Journal of Cell Science* **115**, 1345–1354.

Waters, M. T., Gutjahr, C., Bennett, T., and Nelson, D. C. (2017): Strigolactone signaling and evolution. *Annual Review of Plant Biology* **68**, 291–322.

Waters, M. T., Scaffidi, A., Flematti, G. R., and Smith, S. M. (2012): Karrikins force a rethink of strigolactone mode of action. *Plant Signaling & Behavior* **7**, 969–972.

Wickstead, B., and Gull, K. (2011): The evolution of the cytoskeleton. *J Cell Biol* 194, 513–525.

Wilkins, K. A., Poulter, N. S., and Franklin-Tong, V. E. (2014): Taking one for the team: self-recognition and cell suicide in pollen. *J Exp Bot* **65**, 1331–1342.

Wloga, D., Joachimiak, E., and Fabczak, H. (2017): Tubulin post-translational modifications and microtubule dynamics. *International Journal of Molecular Sciences* **18**, 2207.

Xie, Y., Liu, Y., Ma, M., Zhou, Q., Zhao, Y., Zhao, B., et al. (2020): *Arabidopsis* FHY3 and FAR1 integrate light and strigolactone signaling to regulate branching. *Nature Communications* **11**, 1955.

Xuan, Y., Zhou, S., Wang, L., Cheng, Y., and Zhao, L. (2010): Nitric oxide functions as a signal and acts upstream of AtCaM3 in thermotolerance in *Arabidopsis* seedlings. *Plant Physiology* **153**, 1895–1906.

Yokota, T., Sakai, H., Okuno, K., Yoneyama, K., and Takeuchi, Y. (1998): Alectrol and orobanchol, germination stimulants for *Orobanche minor*, from its host red clover. *Phytochemistry* **49**, 1967–1973.

Yoneyama, K., Akiyama, K., Brewer, P. B., Mori, N., Kawano-Kawada, M., Haruta, S., et al. (2020): Hydroxyl carlactone derivatives are predominant strigolactones in *Arabidopsis*. *Plant Direct* 4, e00219.

Yoneyama, K., Xie, X., Kusumoto, D., Sekimoto, H., Sugimoto, Y., Takeuchi, Y., et al. (2007): Nitrogen deficiency as well as phosphorus deficiency in *Sorghum* promotes the production and exudation of 5-deoxystrigol, the host recognition signal for arbuscular mycorrhizal fungi and root parasites. *Planta* **227**, 125–132.

Zhang, C., Mallery, E., Reagan, S., Boyko, V. P., Kotchoni, S. O., and Szymanski, D. B. (2013): The Endoplasmic Reticulum is a reservoir for WAVE/SCAR regulatory complex signaling in the *Arabidopsis* leaf. *Plant Physiology* **162**, 689–706.

Zhang, R., Alushin, G. M., Brown, A., and Nogales, E. (2015): Mechanistic origin of microtubule dynamic instability and its modulation by EB proteins. *Cell* **162**, 849–859.

Zhou, F., Lin, Q., Zhu, L., Ren, Y., Zhou, K., Shabek, N., et al. (2013): D14–SCF D3 -dependent degradation of D53 regulates strigolactone signalling. *Nature* **504**, 406–410.

Zou, M., Ren, H., and Li, J. (2019): An auxin transport inhibitor targets villin-mediated actin dynamics to regulate polar auxin transport. *Plant Physiol.* **181**, 161–178.

Zwanenburg, B., and Pospíšil, T. (2013): Structure and activity of strigolactones: new plant hormones with a rich future. *Molecular Plant* **6**, 38–62.

8. LIST OF ABBREVIATIONS

ABA	abscisic acid
ABPs	actin-binding proteins
ADF	actin-depolymerizing factors
ADP	adenosinediphosphate
AF	actin filaments
AIP1	actin-interacting protein 1
ARA7	ARABIDOPSIS RAB GTPASE HOMOLOG F2B
Arp2/3	actin-related 2/3 complex
ATD27	*A. thaliana* homolog of rice D27
AtMPB2C	homolog of MPB2C in *Arabidopsis thaliana*
ATP	adenosinetriphosphate
BFA	brefeldin A
CAP	cysteine-rich secretory protein
CCD	carotenoid-cleavage dioxygenase
CISA-1	cyano-isoindole SL analogue
CLA	carlactonic acid
CLASPs	cytoplasmic linker-associated proteins
CLSM	Confocal Laser Scanning Microscopy
Col-0	Wild Type Ecotype of *Arabidopsis thaliana*
CP	capping proteins
D14	DWARF14, A*rabidopsis* analogue At27, petunia
D27	DWARF27, At(14) *Arabidopsis* analogue DAD2 and pea RMS4
D53	DWARF53
DAPI	4',6-diamidino-2-phenylindole
der1	DEFORMED ROOT HAIRS 1
DNA	Deoxyribonucleic acid
EB1	end-binding-1 protein
epi-5DS	5-Deoxystrigol
eir1	ethylene insensitive root 1
ER	endoplasmic reticulum
FABD2-GFP	F-actin binding domain fused with GFP
FtsZ	filamenting temperature-sensitive mutant Z
GDP	Guanosindiphosphate
GTP	Guanosintriphosphate
GFP	green fluorescent protein
GR24	(rac)-GR24, exogenously applied artificial strigolactone
1′-HO-MeCLA	hydroxymethyl carlactonoate
JA	jasmonic acid
KASH	Klarsicht/Anc/Syne-1 homology protein
KAI2	KARRIKIN INSENSITIVE 2
LBO	lateral branching oxidoreductase
MAPs	microtubule associated proteins
MAX	MORE AXILLARY BRANCHES
MBD	microtubule-binding domain
MEB55	SL analogue
MeJA	methyl jasmonate
MeSA	methyl salicylate
MES	2-(N-morpholino)ethanesulfonic acid

MS	Murashige and Skoog
MT	microtubules
PILZ	protein from *Pseudomonas aeruginosa*
PIN	PIN-FORMED (PIN) protein family of auxin transporters
PPF	photosynthetic photon flux
PR	PATHOGENESIS RELATED
PM	plasmatic membrane
PTMs	post-translational modifications
RepX	Plasmid replication protein RepX
SA	salicylic acid
SD	Spinning Disk
Skp	Cullin, F-box (SCF)-containing complex
SL	strigolactones
SMXL	SUPPRESSOR OF MAX2 1-LIKE
SPIRAL1	SPR1 in *Arabidopsis*
ST362	SL analogue
SUN	SAD1/UNC84
TALIN-GFP	GFP fused to the actin binding domain of mouse talin
TIS108	6-phenoxy-1-phenyl-2-(1H-1,2,4-triazol-1-yl) hexan-1
TIS13	2,2-dimethyl-7-phenoxy-4(1H-1,2,4-triazol-1-yl)heptan-3-ol
tir3	TRANSPORT INHIBITOR RESPONSE
TUA6	Tubulin α-6
TubZ	tubulin-like protein
γ-TuRC	γ-tubulin ring complex
WT	Wild Type

9. SUPPLEMENTARY

Supplementary 1

A) B)

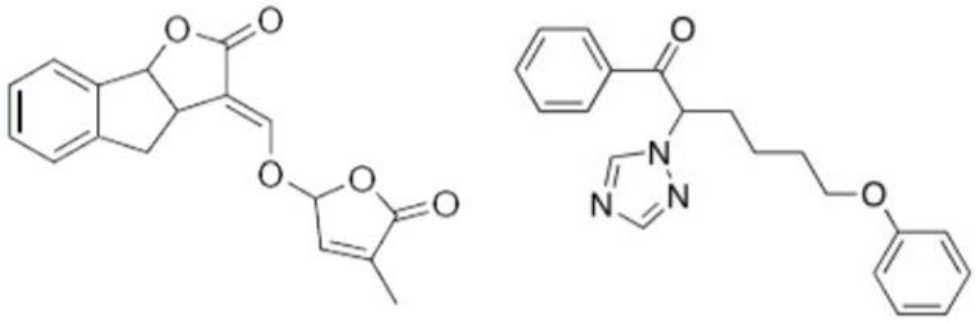

(A) synthetic analogue of strigolactone GR24 (Steinkellner et al., 2007) (rac)-GR24 or [(3aR*,8bS*,E)-3-(((R*)-4-methyl-5-oxo-2,5-dihydrofuran-2-yloxy)methylene)-3,3a,4,8b-tetrahydro-2H-indeno[1,2-b]furan-2-one];

(B) Strigolactone biosynthesis inhibitor TIS108 (Shinsaku et al., 2013) or 6-phenoxy-1-phenyl-2-(1H-1,2,4-triazol-1-yl) hexan-1-one.